Journal of Iberian Geology
https://doi.org/10.1007/s41513-025-00299-5

RESEARCH PAPER

Palynological trends and sedimentological framework of a Barremian estuarine and barrier-island system in the western Tethys (Camarillas Formation, eastern Spain)

Eduardo Barrón[1] · Rocío Navarrete[2] · Juan Pedro Rodríguez-López[2,3,4] · Ana R. Soria[2] · Luis Lassaletta[5] · Carlos L. Liesa[2]

Received: 21 February 2025 / Accepted: 15 May 2025

Abstract

The Early Cretaceous Camarillas Formation represents a thick and extensive estuarine and barrier island-lagoonal depositional system that developed in the Western Tethys (Iberian Basin, eastern Spain). Thirty-seven percent (7 out of 19) of the palynological samples collected from three stratigraphic sections of this formation (six from the sedimentary stage 2 and one from the stage 3) were productive, containing well-preserved palynological assemblages, including 105 taxa. Despite having similar facies to the productive ones, the remaining 63% of the samples were barren of palynomorphs, suggesting that environmental conditions, rather than taphonomical bias, played a key role in preservation. In general, gymnosperm pollen grains and fern spores dominate the palynoflora. Scarce angiosperm pollen grains and aquatic palynomorphs also occur. The most representative taxon in the studied levels is *Classopollis obidosensis*. Angiosperm pollen predominates in the uppermost productive level, whereas the *Cyathidites*/*Deltoidospora* spore-type abounds in a basal one. The palynological study confirms a Barremian age for the Camarillas Formation and provides insights into vegetation mosaics that included conifer-forests along the western Tethyan coasts. However, the data suggest a palaeofloristic change throughout the succession. Firstly (Stage 2), it is characterized by the alternation between xerophytic conifer-woodlands that developed in arid and/or coastal areas and freshwater swamps containing taxodioids and ferns. Then (Stage 3), gymnosperm-producers of the pollen type *Cycadopites*/*Monosulcites* and pioneer angiosperms inhabited brackish swamps.

Keywords Palynology · Biostratigraphy · Barremian · Early Cretaceous · Western Tethys · Iberian Range

Resumen

La Formación Camarillas (Cretácico Inferior, Cuenca Ibérica, este de España) representa un sistema deposicional de estuario e isla barrera-lagoon, potente y extenso, que se desarrolló en el Tethys Occidental. El 37% (7 de 19) de las muestras palinológicas recogidas en tres secciones estratigráficas de esta formación (seis en la Etapa Sedimentaria 2 y una en la Etapa 3 de esta unidad) fueron productivas desde un punto de vista palinológico, presentando asociaciones bien preservadas que permitieron la identificación de 105 taxones. El 63% restante de las muestras carecían de palinomorfos, a pesar de tener

✉ Eduardo Barrón
e.barron@igme.es

Rocío Navarrete
rocionavarrete@iespilarlorengar.com

Juan Pedro Rodríguez-López
drjuampe@unizar.es

Ana R. Soria
anasoria@unizar.es

Luis Lassaletta
luis.lassaletta@upm.es

Carlos L. Liesa
carluis@unizar.es

[1] Museo Geominero, Instituto Geológico y Minero de España (IGME-CSIC), Ríos Rosas 23, 28003 Madrid, Spain

[2] Grupo GEOtransfer, Departamento de Ciencias de la Tierra, Facultad de Ciencias, Instituto de Ciencias Ambientales (IUCA), Universidad de Zaragoza, Pedro Cerbuna 12, 50009 Zaragoza, Spain

[3] Fundación ARAID, Avda. de Ranillas, 50018 Zaragoza, Spain

[4] Permafrost Laboratory, Department of Geography, University of Sussex, Sussex House, Falmer Brighton BN1 9RH, UK

[5] CEIGRAM - Universidad Politécnica de Madrid, Senda del Rey 13, 28040 Madrid, Spain

Published online: 07 June 2025

facies similares a las productivas, lo que sugiere que las condiciones ambientales jugaron un papel clave en la conservación más que el sesgo tafonómico. En general, la palinoflora está caracterizada por granos de polen de gimnospermas, esporas de helechos y, en menor medida, por granos de polen de angiospermas y palinomorfos acuáticos. El taxón más representativo en los niveles estudiados fue *Classopollis obidosensis*, pero en el nivel productivo más alto predomina el polen de angiospermas, mientras que esporas del tipo *Cyathidites*/*Deltoidospora* abundan en un nivel basal. El estudio palinológico confirma una edad Barremiense para la Formación Camarillas y proporciona información sobre la existencia de mosaicos de vegetación que incluían el desarrollo de bosques de coníferas a lo largo de las costas occidentales del Tethys. Sin embargo, los datos sugieren un cambio paleoflorístico a lo largo de la sucesión; en primer lugar (Etapa 2), caracterizado por la alternancia de formaciones xerofíticas de coníferas propias de ambientes áridos y/o costeros y pantanos de agua dulce poblados por taxodioides y helechos, y luego (Etapa 3) por pantanos salobres donde crecieron gimnospermas productoras del tipo polínico *Cycadopites*/*Monosulcites* y angiospermas de carácter pionero.

Palabras clave Palinología · Bioestratigrafía · Barremiense · Cretácico Inferior · Tethys occidental · Cordillera Ibérica

1 Introduction

Palynological studies from the Barremian of the Tethys realm are scarce and often yield variable results. Although an almost continuous plant macrofossil record exists for the Early Cretaceous of Iberia (Diéguez et al., 2010), Barremian palynofloras remain poorly documented in the Iberian Peninsula. Only a few incomplete palynological studies have been carried out in Barremian strata (Médus, 1970; Pais & Reyre, 1980–1981; Doubinger & Mas, 1981; Taugourdeau-Lantz, 1988; Leereveld et al., 1989; Sole de Porta & Salas, 1994; Friis et al., 2000, 2011; Villanueva-Amadoz et al., 2014; De la Fuente & Zetter, 2016; Mendes et al., 2018, 2023; Rodríguez-Barreiro et al., 2024).

The studied samples presented here have been collected from the Barremian Camarillas Formation in the Galve Sub-basin (Iberian Basin, Spain). The first palynological information from this sub-basin was published by Mohr (1987, 1989), who studied only a single assemblage collected near the village of Galve. The assemblage contained a high percentage of the so-called *Corollina*/*Sph eripollenites*/*Exesipollenites* complex (47.5%), large trilete spores (37.5%), and punctual presence of the angiosperm pollen *Clavatipollenites hughesii*. Recently, Pons et al. (2013) and Villanueva-Amadoz et al. (2015) studied three assemblages of the Camarillas Formation near the same locality providing a list of palynological taxa.

Despite existing palynological studies, a comprehensive analysis of the Camarillas Formation remains to be conducted. The present study aims to address this deficiency by providing a detailed palynological characterization across three stratigraphic sections in the Galve Sub-basin (Teruel, eastern Spain). This palynological investigation is accompanied by a detailed sedimentological analysis of the sedimentary facies encompassing the palynological sampling locations. The deposition of the Camarillas Formation in transitional environments (Soria et al., 2023) presents a valuable opportunity to examine Barremian southwestern European Tethyan floras. The outcomes of this research allow for the refinement of its biostratigraphic framework and dating, as well as the reconstruction of the palynological trends and palaeoenvironmental conditions that characterized this region during the Early Cretaceous. These results are discussed in relation to previous Iberian findings to elucidate palaeoenvironmental trends and their causal factors.

2 Geological setting

The studied area is located in the Iberian Range, a NW–SE intraplate fold-and-thrust belt formed by the tectonic inversion of the Mesozoic Iberian basins during the Cenozoic (Álvaro et al., 1979; Capote et al., 2002; Liesa et al., 2018; Martín-Chivelet et al., 2002; Salas & Casas, 1993; Simón & Liesa, 2011). More specifically, the Galve Sub-basin is one of these extensional Mesozoic Iberian basins (Fig. 1a, b). This sub-basin was differentiated during the Late Jurassic–Early Cretaceous rifting stage (Fig. 1c), which affected the Iberian Plate and led to the fragmentation of the marine platforms and ramps that characterized the Jurassic sedimentation (Capote et al., 2002; Liesa et al., 2019; Salas & Casas, 1993; Soria, 1997; Soria et al., 2000).

The extensional structure of the Galve Sub-basin (Fig. 1b, d) is characterized by a NNW-SSE trending graben that is limited by NNW-SSE trending and steep normal faults and is compartmentalized by a set of ENE-WSW listric normal faults resulting in a system of minor half-grabens and grabens (Liesa et al., 2000, 2004, 2006; Meléndez et al., 2009; Soria, 1997; Soria et al., 2001). The synrift series, specially the early units, displays great thickness variations in relation with these Mesozoic faults (e.g., Aurell et al., 2016; Liesa et al., 2004, 2006, 2023; Navarrete et al., 2013a). Differential subsidence driven by normal faults was encompassed by general uplift related to doming processes in eastern Iberia, especially during the Berriasian–Hauterivian (Antolín-Tomás et al., 2007; Liesa et al., 2019). As a result, sedimentation was firstly restricted to depocentral areas of

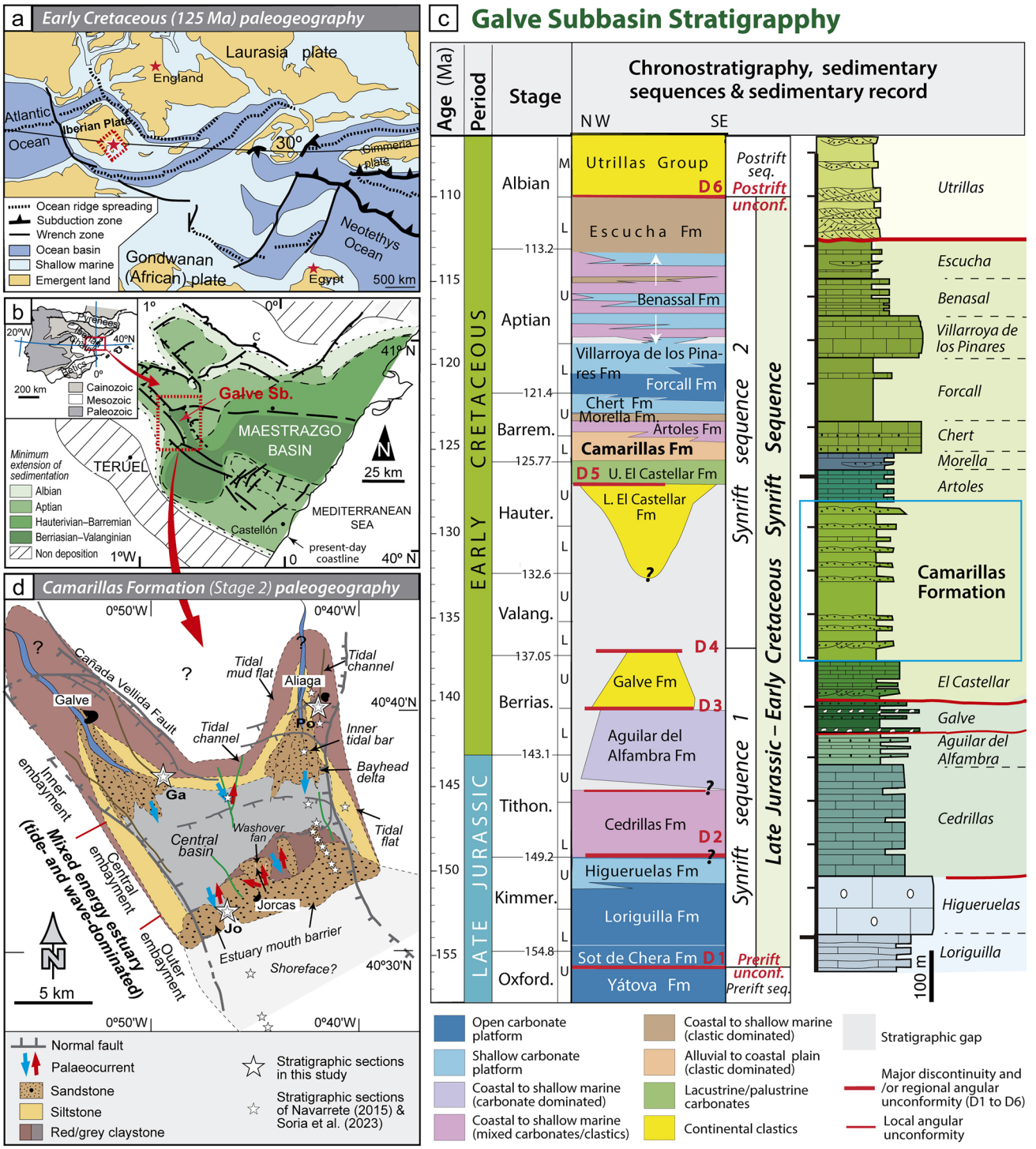

Fig. 1 Geological setting of the Camarillas Formation in the Galve Sub-basin. **a** Early Cretaceous (125 Ma) palaeogeographical sketch of the western Tethys Sea showing the location of the Galve Sub-basin in eastern Iberia (dashed rectangle), England and Egypt (stars) (modified from Blackey, 2014). **b** Location of the Galve sub-basin in western Maestrazgo Basin, eastern Iberia, and major extensional faults (modified from Capote et al., 2002). **c** Chronostratigraphy (modified from Liesa et al., 2019; Aurell et al., 2019 and updated to the Geological Time Scale of Gale et al., 2020) and sedimentary record of the Galve Sub-basin (modified from Liesa et al., 2023). **d** Palaeogeography of the Stage 2 (mixed estuary) of the Camarillas Formation in the Galve Sub-basin (after Soria et al., 2023). Small stars: sections used by Soria et al. (2023) to interpret the sedimentology and palaeogeography. Big stars: stratigraphic sections studied here (Jo: Jorcas, Po: La Porra, Ga: Galve)

subbasins (synrift series 1; Fig. 1c), dominated by shallow marine to coastal environments (Cedrillas and Aguilar del Alfambra formations) during the latest Jurassic, and mostly terrestrial ones (Galve Formation) during the earliest Cretaceous (Aurell et al., 2016, 2019; Liesa et al., 2019, 2023). Conversely, the areas between basins and sub-basins experienced fault block tilting and differential erosion. During the Early Cretaceous, tectonic subsidence together with high sea level gave rise to a progressive connection between sub-basins, and the development of local and regional synrift (and intrarift) angular unconformities (Liesa et al., 2019). The Early Cretaceous synrift sedimentation of the Galve Sub-basin (synrift series 2; Fig. 1c) extends from the late Hauterivian to the early-middle Albian (Aurell et al., 2016; Peropadre, 2012; Salas, 1987; Salas et al., 2001; Soria, 1997; Soria et al., 2000). It mainly comprises (Fig. 1d): (1) alluvial and lacustrine series of the El Castellar Formation (Illueca et al., 2023, 2024; Liesa et al., 2004, 2006; Meléndez et al., 2009; Soria, 1997); (2) red claystones and sandstones of the Camarillas Formation (Soria, 1997), which has been recently interpreted as deposited in transitional environments (estuary and barrier island-lagoonal systems) (Navarrete et al., 2013b; Soria et al., 2023); (3) marlstones and limestones of the Artoles Formation, interpreted as shallow marine carbonates (Ibáñez et al., 2015; Salas, 1987; Soria, 1997), and (4) a series of mixed siliciclastic-carbonate marine platforms, represented by the Morella, Chert, Forcall, Villarroya de los Pinares, and Benassal formations (Bover-Arnal, 2010; Peropadre, 2012; Peropadre et al., 2007, 2008, 2013; Salas et al., 2001). The Early Cretaceous synrift stage ended with an increase in extensional activity and sedimentation of coastal mudstones and sandstones with coal (the Escucha Formation; Rodríguez-López, 2008; Rodríguez-López et al., 2009).

3 Material and methods

The palynological samples were recovered from three different stratigraphic profiles of the Camarillas Formation namely the Jorcas (Jo), La Porra (Po), and Galve (Ga) sections. These stratigraphical sections are located in the western, northeastern and northwestern sectors of the Galve Sub-basin, respectively (Fig. 1d). The stratigraphy and sedimentology of the Camarillas Formation has been based on the detailed study of 19 complete stratigraphic sections (with a total logged thickness of > 5.6 km) logged across the Galve Sub-basin (Fig. 1d) (Navarrete, 2015; Navarrete et al., 2013a, 2013b, 2014; Soria et al., 2023). The sedimentological and stratigraphic studies were assisted by the analysis of 1:18,000 scale aerial photographs, high-resolution (0.5 m/pixel) colour aerial orthoimages, and detailed aerial photographs taken from a drone device (see Navarrete et al., 2013a, 2013b, 2014; Soria et al., 2023).

Nineteen samples were taken from different black to gray organic-rich levels across the three stratigraphic sections, but only seven (37%) yielded palynological content. Samples were processed following the standard palynological technique (Batten, 1999; Traverse, 2007), i.e., acid treatment with HCl, HF and HNO_3 at high temperature. The residues were concentrated using 500, 250, 75, 50 and 12 µm sieves. Samples were mounted in glycerine jelly and examined by light microscopy using an Olympus BX51 optical microscope. All samples were prepared at the ALICONTROL laboratory (Madrid, Spain). The prepared slides and residues are provisionally stored at the Museo Geominero, Instituto Geológico y Minero de España—IGME-CSIC, Madrid. At least 300 palynomorphs were examined for each sample to determine species ratios. A pollen diagram was constructed using Tilia and TGView 2.0.2 software (Grimm, 1992, 2004) to determine the quantitative variation in taxa over the succession.

A Correspondence Analysis (CA) (Benzécri, 1973) was performed in order to explore the common variance of the different levels according to their similarities in their taxa abundance. This multivariate ordination method has been successfully employed in many palaeoecological studies of the Mesozoic (Barrón et al., 2010, 2023; Peyrot et al., 2007; Wagstaff et al., 2006). We first performed a CA including 7 levels and 15 taxa. To do so the matrix was conditioned, grouping some taxa and avoiding the inclusion of rare taxa that produce noise in ordination analyses. The taxa with the best quality of representation were mainly considered (i.e., those with the highest absolute and relative contributions). Undetermined spores and *Spheripollenites* grains were not considered because their attribution to gymnosperms is sometimes disputed (Barrón et al., 2010). A second CA analysis with a smaller matrix (5 levels × 15 taxa) was conducted to unveil the variability among the most similar levels.

4 Results

4.1 Stratigraphy and sedimentology: the Camarillas Formation

In the Galve Sub-basin, the Camarillas Formation lies on the Lower Barremian lacustrine marlstones and limestones of the El Castellar Formation (Canudo et al., 2012; Gasca, 2015; Illueca et al., 2024; Meléndez et al., 2009; Soria, 1997), and is covered by the marlstones, limestones and occasional sandstones of the late Barremian lagoonal facies of the Artoles Formation (Ibáñez et al., 2015; Soria, 1997) (Fig. 1c).

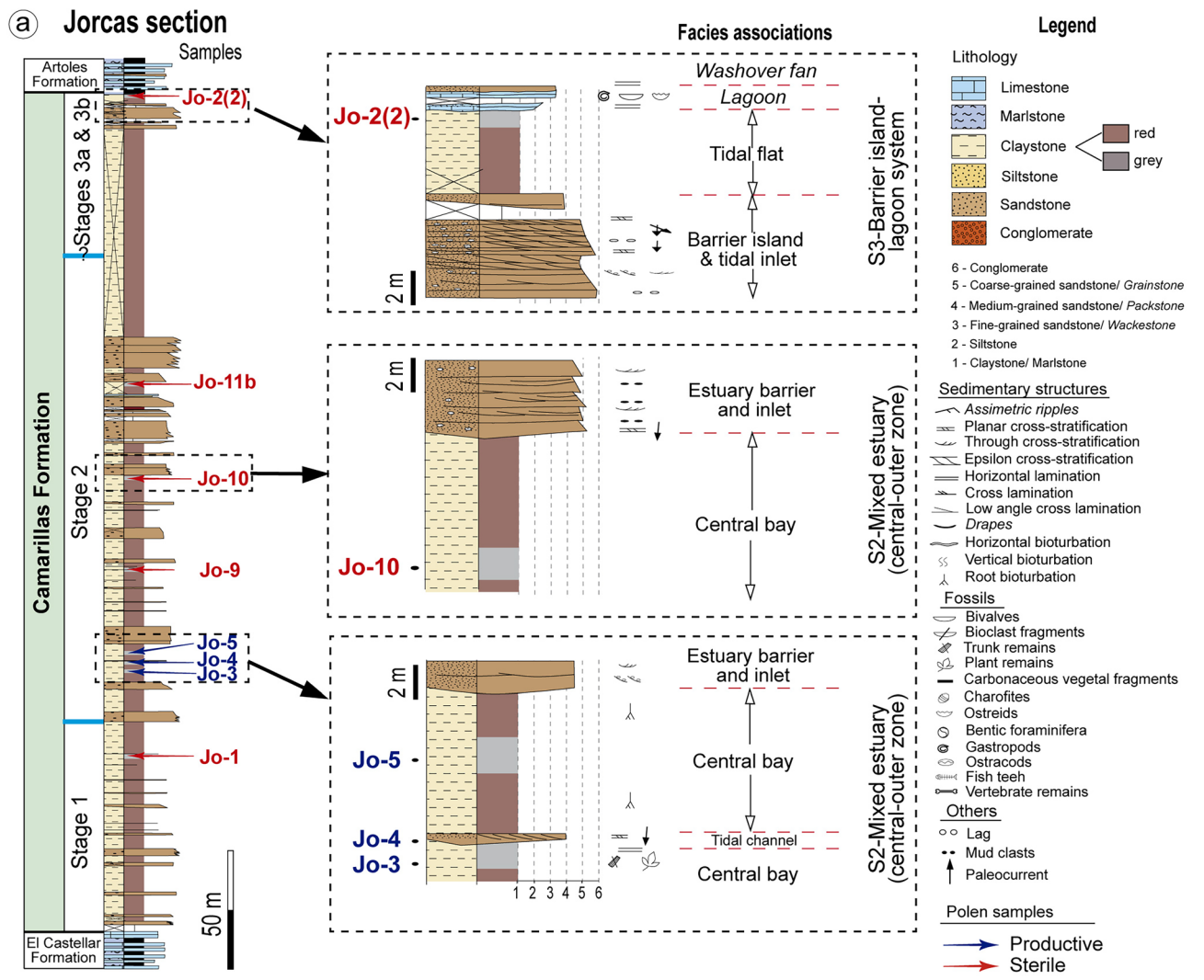

Fig. 2 The Jorcas (Jo) section. **a** Jorcas profile with the location of samples collected for this study and detailed stratigraphic sections showing facies associations, lithofacies, sedimentary structures and palaeocurrent data. **b** Field view of the claystone beds, interpreted as tidal mud flat deposits in the outer estuary (see Fig. 1d), where samples Jo-3, 4 and 5 were collected

The Camarillas Formation consists of m- to dm-thick intervals of dark-red and grey claystones, interbedded dm- to m-thick white and ochre sandstones, and occasional grey marlstones and limestones (Figs. 2, 3, 4). It contains a great variety of vertebrate fauna as dinosaur and shark teeth (e.g., Canudo & Cuenca, 1996; Ruiz-Omeñaca et al., 2004; Badiola et al., 2011; Navarrete et al., 2014) and charophytes, gastropods, oysters and ostracods (e.g.,

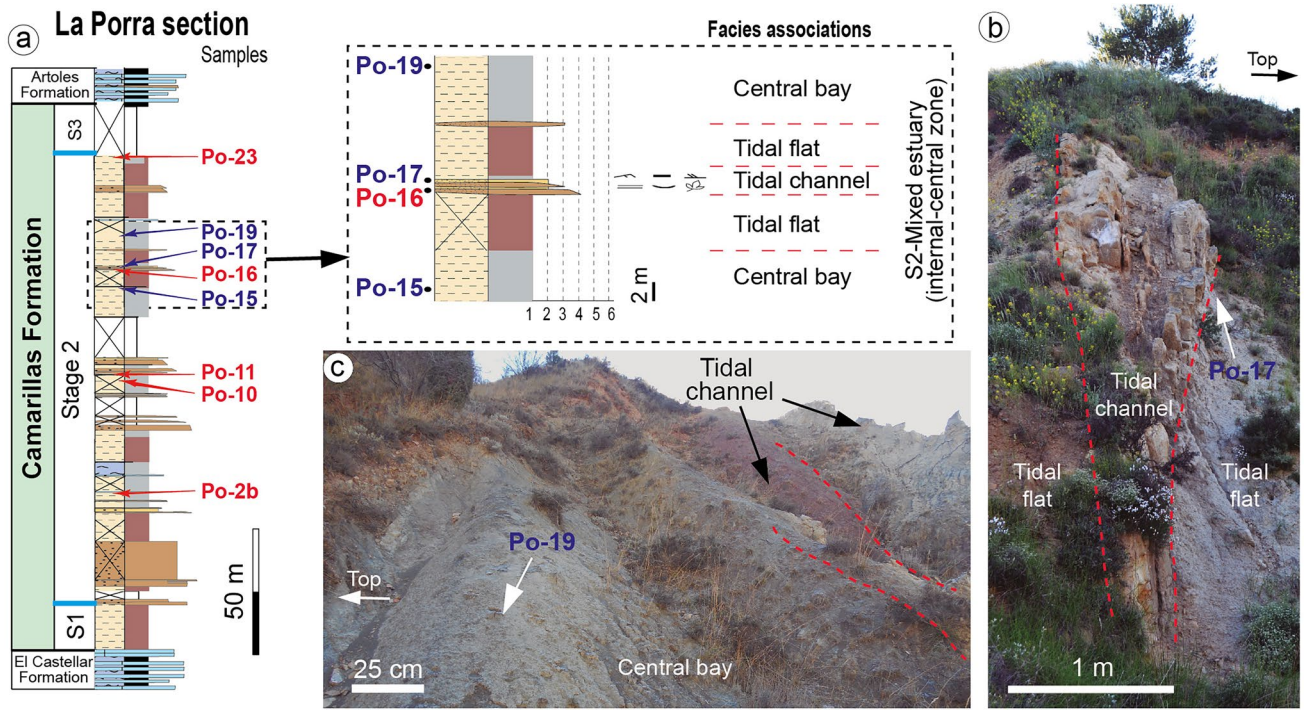

Fig. 3 The La Porra (Po) section. **a** La Porra profile showing samples location and detailed stratigraphic sections with the interpreted facies associations (legend as in Fig. 2). **b** Field view of the grey mudstone beds, above and below a sandstone level, where samples Po-15 and Po-17 were collected, representing tidal mud flats and an interbedded tidal channel deposit at the inner part of the estuary (see Fig. 1d). **c** Field view of grey mudstone beds sampled in Po-19

Martín-Closas, 1989; Schudack & Schudack, 2009; Soria, 1997). This formation shows a variable thickness, ranging from 300 to 1000 m in the Galve Sub-basin, as it accumulated during the Late Jurassic–Early Cretaceous rift climax stage (Navarrete, 2015; Navarrete et al., 2013a; Soria et al., 2023). This period was characterized by maximum subsidence rates with high spatial variability. Deposition developed under the influence of usually blind normal growth faults as is deduced by the absence of the typical slope facies associated to scarps on master faults (e.g., Navarrete et al., 2013a, 2013b, 2014).

Classical sedimentological interpretations of the Camarillas Formation regard the sedimentation in the Galve Sub-basin as taking place in coastal fluvial systems with tidal influence towards the unit top (e.g., Díaz Molina & Yébenes, 1987; Salas, 1987; Soria, 1997). Recent investigations on a basin scale have allowed us to proposed a sedimentary evolution for this unit consisting into three main stages (S1 to S3; Fig. 5) including barrier island and estuary systems (Navarrete, 2015; Navarrete et al., 2013b, 2014; Soria et al., 2023). According to Soria et al. (2023), Stage-1 is constituted by a tide-dominated estuary with a basal fluvial system; Stage-2 is a mixed tide- and wave-dominated estuary (Fig. 1d), and Stage 3 is a barrier island-lagoonal system, which has been divided into two parts (stages 1 and 2 of Navarrete et al., 2013b) according to the evolution of the mixed siliciclastic-carbonate back-barrier systems.

4.2 Stratigraphic sections and sample location

As mentioned above, three stratigraphic sections of the Camarillas Formation have been studied in the present study (Fig. 1d): the Jorcas, Galve and La Porra sections.

The Jorcas (Jo) section is located in a valley between Jorcas and Allepuz localities, about 4 km northwest of the village of Allepuz (Fig. 1d). In this outcrop the Camarillas Formation is 367 m thick and is constituted by thick intervals of dark-red and grey claystones and interbedded cm- to m-thick dark-red and white/ochre sandstones (Fig. 2a). The top of the unit displays m- to cm-thick grey marlstones and limestones. Eight samples were collected along the section selecting organic-rich grey claystone levels (Fig. 2b). The three productive samples (marked in blue colour in Fig. 2a) were taken from an interval of massive m-thick grey-black and dark-red mudstones and interbedded dm-thick grey-white sandstones from the middle-lower part of the section (basal part of Stage 2). In particular, samples Jo-3 and Jo-4 were collected in the first grey claystone interval (between 114 and 115.5 m of the section), which shows

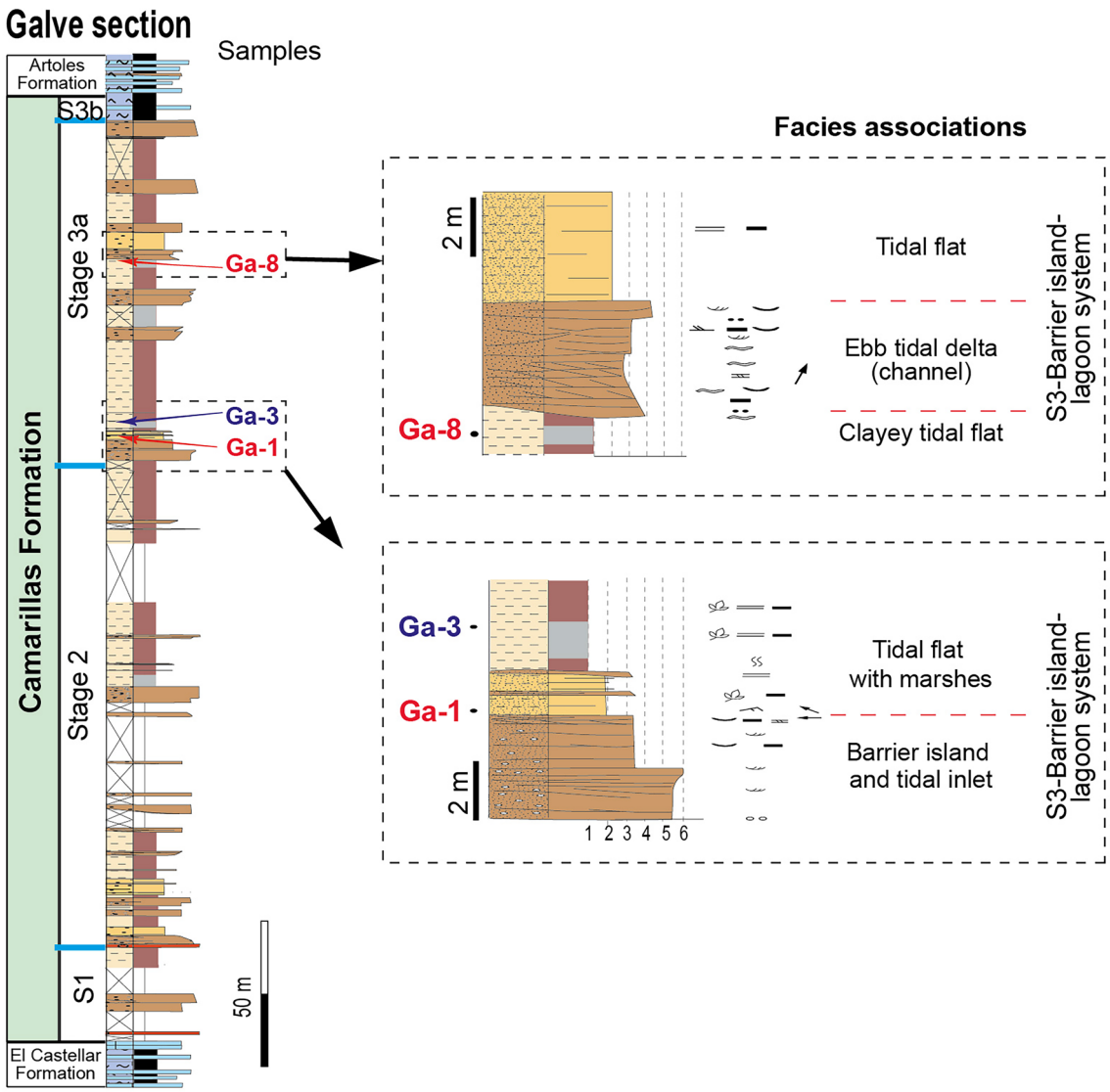

Fig. 4 The Galve (Ga) section (see location in Fig. 1d) with the location of samples and detailed stratigraphic sections with the distinguished facies associations (legend as in Fig. 2)

parallel lamination and contains trunk and plant remains (Fig. 2a, b). Sample Jo-5 was collected at the top of the interval (at 119.5 m), a 1.5 m-thick massive grey claystone level (Fig. 2a). These claystone levels have been interpreted as accumulated in a shallow central embayment of a closed or semi-enclosed estuary forming extensive back-barrier muddy tidal flats in the outer embayment (Fig. 1d) (Navarrete, 2015; Soria et al., 2023). The fine–grained particles settled out from suspension under conditions of very low energy; the presence of vegetation associated with supratidal and intertidal areas in back–barrier systems is very common (e.g. Davis et al., 2003).

The La Porra (Po) section is located in a gully close to the Aliaga village (Fig. 1d). Here, the 180 m thick Camarillas Formation is also constituted by thick intervals of dark-red and grey claystones and interbedded m- to cm-thick red and white/ochre sandstones (Fig. 3). Occasional intercalations of dm- to cm-thick grey marlstone and limestone beds also appear. Eight samples were collected along the section (Fig. 3a). The three samples that yielded palynological assemblages are located in the middle-upper part of the section (upper part of Stage 2); an interval formed by tabular m-thick dark-red and grey-black claystones levels and interbedded m- and cm-thick white sandstones packages. In particular, sample Po-15 was taken in a tabular 12 m-thick grey claystone level with parallel lamination (between meter 91 and 92; Fig. 3a). Sample Po-17 was taken in a 50 cm-thick siltstone level, located at the top of a m-thick grey sandstone package (Fig. 3a, b). Siltstones show parallel lamination, abundant carbonaceous plant remains, coal fragments and

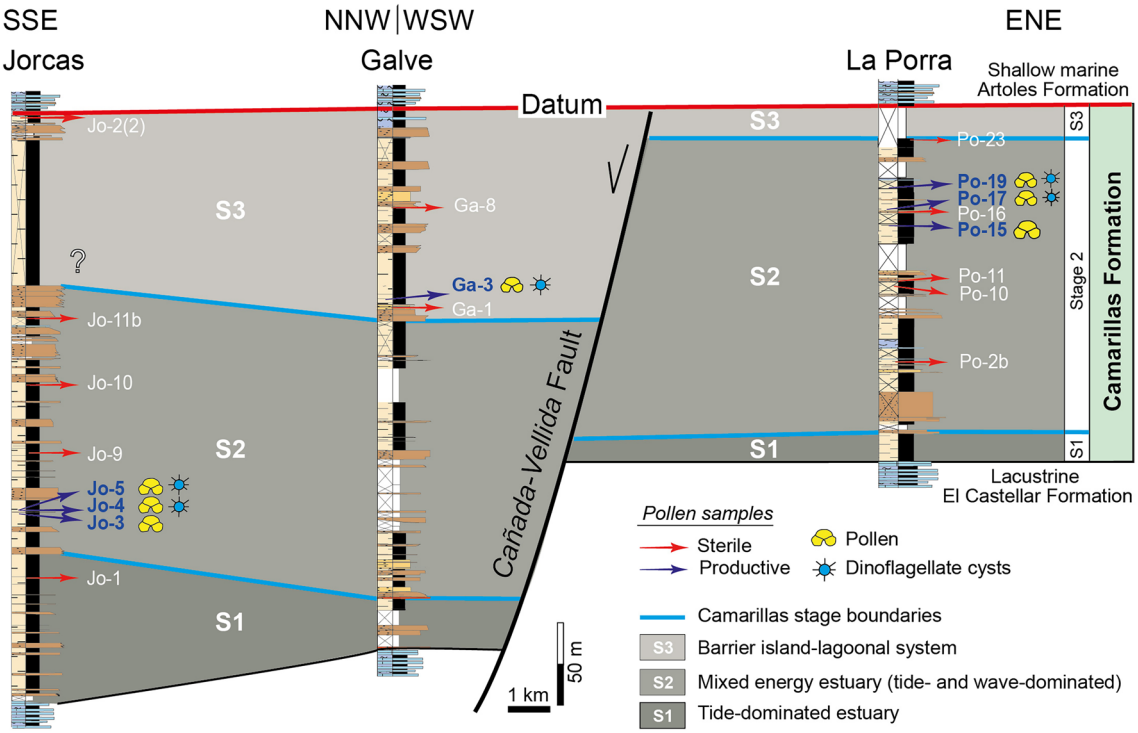

Fig. 5 Correlation panel of the stratigraphic sections and pollen samples. The three stages of the sedimentary evolution distinguished by Navarrete (2015) and Soria et al. (2023) for the Camarillas Formation in the Galve Sub-basin have been included. Note as the NNW-SSE trending Cañada Vellida normal fault was mainly active during the Stage 3, as suggested by the change in thickness

carbonaceous drapes. Sample Po-19 is located at the top of a massive 6 m-thick grey claystone level (Fig. 3c). Po-15 and Po-19 were collected in levels interpreted as the central basin, closed to the inner part of an estuary (Navarrete et al., 2013b; Soria et al., 2023). On the other hand, Po-17 was collected in the upper part of a tidal creek (inter-subtidal region) of the inner estuary surrounded by tidal mud flats.

The Galve (Ga) profile is situated about 4 km southeast of the Galve village (Fig. 1d). The Camarillas Formation in this outcrop is 336.5 m thick and comprises m- to cm-thick white/ochre sandstone levels interbedded with thick dark-red and grey claystone intervals (Fig. 4). The top of the section is a dm- to cm-thick grey limestone interval. The three investigated samples were collected in the middle-upper part of the section (basal part of Stage 3). Only the sample Ga-3 yielded a representative palynological assemblage. It was collected at the top of a 2.5 m-thick grey claystone level (between 209.5 and 211 m), showing parallel lamination, carbonaceous plant remains and abundant organic matter (Fig. 4). This interval containing plant remains has been interpreted as a back-barrier marsh developed in association with a tidal mud flat (Navarrete et al., 2013b; Soria et al., 2023).

Figure 5 displays the stratigraphic correlation of the studied sections of the Camarillas Formation in the Galve Sub-basin indicating the relative stratigraphic location of the studied palynological samples. As a whole, seven sedimentary levels – 3 from the Jorcas section, 3 from the La Porra section and 1 from the Galve section – yielded representative and well-preserved palynological assemblages. Levels are mainly located at the embayment grey claystone deposits of the mixed estuary of the Stage 2: three in its lower part (at Jorcas section) and three in its upper part (La Porra section). The level inferred at Galve is located at the lower part of the barrier island-lagoon system of Stage 3.

4.3 Palynological study

A total of 105 taxa have been identified from the study of the seven palynological samples described above (Table 1; Appendix 1). These taxa include bryophytic and vascular cryptogram spores (Figs. 6, 7), pollen grains of gymnosperms (Fig. 8a–k, m, p–s, x) and angiosperms (Fig. 8l, n–o, t–w), and aquatic palynomorphs (Fig. 6a–b, s). Miospores are predominant in all the samples analysed (Fig. 9); 67 spore taxa and 31 pollen types (26 gymnosperms and 5 angiosperms) were found. The spores of vascular cryptogams are the most diverse group (see Figs. 6, 7). However, all studied levels are dominated by pollen grains of gymnosperms (Fig. 9), except for the level Ga-3, which is characterized by pollen of angiosperms

Table 1 List of palynomorphs identified in the Barremian sediments of the Camarillas Formation organised by their botanical affinities following Barrón et al. (2023) and Pérez-Loinaze et al. (2023)

Taxa	Botanical affinity	General ecology	Jo-3	Jo-4	Jo-5	Po-15	Po-17	Po-19	Ga-3
Aquatic palynomorphs									
Undetermined acanthomorph acritarchs	Acritarcha	**1**	–	r	–	–	–	r	–
Chomotriletes minor	Chlorophyta (Zygnemataceae)	**2**	–	–	–	–	r	–	–
Schizosporis reticulatus (Fig. 6s)	Chlorophyta (Prasinophyte)	**3**	–	–	p	r	–	–	–
Pleurozonaria sp.	Chlorophyta (Prasinophyte)	**1**	–	–	p	–	–	–	–
Chlamidophorella sp. (Fig. 6a)	Dinoflagellata	**3**	–	–	–	–	r	–	–
Cleistosphaeridium sp. (Fig. 6b)	Dinoflagellata	**3**	–	–	–	–	–	–	r
Undetermined dinoflagellate cysts	Dinoflagellata	**3**	–	r	r	–	–	r	–
Miospores									
Spores									
Aequitriradites spinulosus (Fig. 6f)	Hepaticophyta	**4**	–	–	–	r	–	–	–
Aequitriradites verrucosus (Fig. 6e)	Hepaticophyta	**4**	r	–	R	p	p	r	–
Appendicisporites cf. *bilateralis*	Monilophyta (Schizaeales, Anemiaceae)	**5**	–	r	–	–	r	r	–
Appendicisporites tricornitatus	Monilophyta (Schizaeales, Anemiaceae)	**5**	–	r	–	r	–	–	–
Appendicisporites spp. (Fig. 7e)	Monilophyta (Schizaeales, Anemiaceae)	**5**	r	r	–	p	p	–	r
Baculatisporites comaumensis	Monilophyta (Osmundaceae)	**5**	r	r	–	–	–	–	–
Biretisporites potoniaei	Monilophyta (uncertain affinities)	**5**	r	–	r	r	r	r	–
Ceratosporites sp.	Lycophyta (Selaginellaceae)	**5**	r	r	–	r	r	–	–
Cibotiumspora jurienensis	Monilophyta (uncertain affinities)	**5**	–	–	r	–	–	–	r
Cicatricosisporites cf. *apicanalis* (Fig. 7b)	Monilophyta (Schizaeales, Anemiaceae)	**5**	r	p	–	–	r	–	–
Cicatricosisporites cf. *australiensis*	Monilophyta (Schizaeales, Anemiaceae)	**5**	–	–	–	r	r	–	–
Cicatricosisporites brevilaesuratus	Monilophyta (Schizaeales, Anemiaceae)	**5**	–	r	–	–	–	–	–
Cicatricosisporites? *hughesii*	Monilophyta (Schizaeales, Anemiaceae)	**5**	–	r	–	–	–	r	–
Cicatricosisporites cf. *ludbrookiae* (Fig. 7c)	Monilophyta (Schizaeales, Anemiaceae)	**5**	r	–	–	–	–	–	–
Cicatricosisporites minutaestriatus (Fig. 7h)	Monilophyta (Schizaeales, Anemiaceae)	**5**	–	–	–	r	–	–	–
Cicatricosisporites mohrioides	Monilophyta (Schizaeales, Anemiaceae)	**5**	r	–	–	–	–	–	–
Cicatricosisporites potomacensis (Fig. 7f–g)	Monilophyta (Schizaeales, Anemiaceae)	**5**	–	r	–	–	–	–	–
Cicatricosisporites venustus (Fig. 7a)	Monilophyta (Schizaeales, Anemiaceae)	**5**	–	r	r	r	r	–	R
Cicatricosisporites spp.	Monilophyta (Schizaeales, Anemiaceae)	**5**	C	C	R	C	A	C	R
Cingutriletes clavus (Fig. 6h)	Bryophyta (Sphagnales, Sphagnaceae)	**5**	r	r	–	r	r	–	–
Concavissimisporites apiverrucatus (Fig. 7s)	Monilophyta (Dicksoniaceae/ Lygodiaceae)	**5**	–	–	p	–	–	r	–
Concavissimisporites informis (Fig. 7o)	Monilophyta (Dicksoniaceae/ Lygodiaceae)	**5**	r	–	C	r	–	–	–
Concavissimisporites verrucosus	Monilophyta (Dicksoniaceae/ Lygodiaceae)	**5**	–	–	p	r	–	r	R
Concavissimisporites spp.	Monilophyta (Dicksoniaceae/ Lygodiaceae)	**5**	–	r	–	–	r	–	–

Table 1 (continued)

Taxa	Botanical affinity	General ecology	Jo-3	Jo-4	Jo-5	Po-15	Po-17	Po-19	Ga-3
Costatoperforosporites cf. *fistulosus* (Fig. 7d)	Monilophyta (Schizaeales, Anemiaceae)	**5**	r	r	–	r	–	–	–
Costatoperforosporites sp.	Monilophyta (Schizaeales, Anemiaceae)	**5**	–	–	–	–	r	–	–
Cyathidites australis	Monilophyta (uncertain affinities)	**5**	C	R	A	r	R	R	C
Cyathidites minor	Monilophyta (uncertain affinities)	**5**	–	–	–	r	R	R	P
Deltoidospora spp.	Monilophyta (uncertain affinities)	**5**	p	p	C	p	R	C	R
Densoisporites velatus	Lycophyta (Pleuromeiaceae?)	**2, 5**	r	r	–	r	–	–	–
Dictyophyllidites sp.	Monilophyta (Dipteridaceae/ Matoniaceae)	**5**	–	–	r	–	–	–	–
Echinatisporis sp.	Lycophyta (Selaginellaceae)	**4**	–	–	–	–	r	–	–
Foraminisporis sp. (Fig. 6c)	Hepaticophyta	**5**	–	r	r	–	r	–	–
Foveosporites cf. *subtriangularis* (Fig. 6o)	Lycophyta	**5**	r	–	–	R	r	–	–
Foveosporites sp. (Fig. 6n)	Lycophyta	**5**	–	–	–	r	r	–	–
Gleicheniidites minor	Monilophyta (Gleicheniaceae)	**4**	–	–	r	–	–	–	–
Gleicheniidites senonicus (Fig. 7m)	Monilophyta (Gleicheniaceae)	**4**	r	r	–	r	–	–	R
Ischyosporites pseudoreticulatus (Fig. 7k)	Monilophyta (Schizaeales, Schizaeaceae)	**5**	r	r	–	r	r	–	–
Leptolepidites macroverrucosus (Fig. 6g)	Lycophyta?	**5**	–	–	–	r	–	–	–
Leptolepidites proxigranulatus (Fig. 6l)	Lycophyta?	**5**	r	p	–	r	p	–	–
Matonisporites phlebopteroides (Fig. 7l)	Monilophyta (Matoniaceae)	**4**	–	r	r	–	–	r	R
Neoraistrickia sp.	Lycophyta (Selaginellaceae)	**4**	r	–	–	–	r	–	–
Nodosisporites cf. *costatus* (Fig. 7i)	Monilophyta (Schizaeales, Anemiaceae)	**5**	–	–	–	r	–	–	–
Osmundacidites wellmanii	Monilophyta (Osmundaceae)	**5**	r	r	r	r	r	–	–
Patellasporites tavaredensis (Fig. 7j)	Monilophyta (uncertain affinities)	**5**	r	p	–	p	r	r	–
Phlebopterisporites sp.	Monilophyta (Matoniaceae)	**4**	–	–	–	r	–	–	–
Pilosisporites trichopapillosus form *brevis*	Monilophyta (uncertain affinities)	**5**	–	–	r	–	–	–	–
Pilosisporites trichopapillosus form *trichopapillosus*	Monilophyta (uncertain affinities)	**5**	r	r	r	R	r	r	–
Pilosisporites verus (Fig. 7r)	Monilophyta (uncertain affinities)	**5**	–	r	r	r	r	r	–
Polycingulatisporites cf. *reduncus* (Fig. 6p)	Bryophyta (Sphagnales, Sphagnaceae)	**5**	r	r	r	r	r	–	–
Polycingulatisporites sp.	Bryophyta (Sphagnales, Sphagnaceae)	**5**	–	–	–	r	–	–	–
cf. *Punctatisporites* sp. (Fig. 7q)	Monilophyta (Marattiaceae?)	**5**	r	r	A	r	r	–	C
Retitriletes cf. *facetus* (Fig. 6m)	Lycophyta (Lycopodiaceae)	**5**	r	–	–	–	r	–	–
Retitriletes reticulumsporites (Fig. 6q)	Lycophyta (Lycopodiaceae)	**5**	–	–	–	p	–	–	–
Retitriletes sp.	Lycophyta (Lycopodiaceae)	**5**	–	–	r	–	–	–	–
Rubinella major (Fig. 6r)	Lycophyta?	**5**	r	r	r	–	–	–	–
Staplinisporites telatus (Fig. 6i)	Lycophyta (Lycopodiaceae)	**5**	–	–	r	r	r	r	–
Stereisporites antiquasporites (Fig. 6j)	Bryophyta (Sphagnales, Sphagnaceae)	**5**	–	–	–	–	–	–	r
Stereisporites aulosenensis	Bryophyta (Sphagnales, Sphagnaceae)	**5**	–	–	–	r	–	–	–
Stereisporites spp. (Fig. 6k)	Bryophyta (Sphagnales, Sphagnaceae)	**5**	r	r	p	r	p	r	r
Todisporites minor	Monilophyta (Osmundaceae)	**5**	–	–	–	r	–	–	–

Table 1 (continued)

Taxa	Botanical affinity	General ecology	Jo-3	Jo-4	Jo-5	Po-15	Po-17	Po-19	Ga-3
Trilobosporites purverulentus (Fig. 7n)	Monilophyta (Lygodiaceae)	**5**	–	–	r	–	–	–	r
Trilobosporites sp.	Monilophyta (Lygodiaceae)	**5**	–	–	p	–	–	–	–
Triporoletes reticulatus (Fig. 6d)	Hepaticophyta (cf. Ricciaceae)	**5**	r	–	r	r	r	–	–
Triporoletes sp.	Hepaticophyta (cf. Ricciaceae)	**5**	–	–	r	–	–	–	–
Undulatisporites spp.	Monilophyta (uncertain affinities)	**5**	r	r	r	r	–	r	–
Verrucatosporites sp. (Fig.)	Monilophyta (uncertain affinities)	**5**	–	–	–	–	–	r	–
Undetermined trilete spores	–	–	r	R	r	p	p	r	–
Pollen grains (gymnosperms)									
Afropollis jardinus	Uncertain affinity	**8**	–	–	–	r	r	–	–
Alisporites bilateralis (Fig. 8a)	Corystospermales? Podocarpaceae?	**6**	R	R	–	p	r	–	p
Alisporites spp.	Corystospermales? Podocarpaceae?	**6**	r	–	–	p	r	–	–
Araucariacites australis (Fig. 8b)	Coniferales, Araucariaceae	**6, 10**	C	C	A	R	C	R	R
Callialasporites dampieri (Fig. 8d)	Coniferales, Araucariaceae	**6, 10**	r	r	r	r	r	r	r
Cedripites cf. *cretaceous* (Fig. 8i)	Coniferales, Pinaceae	**6**	–	–	–	–	–	–	r
Classopollis obidosensis (Fig. 8f–g)	Coniferales, Cheirolepidiaceae	**8, 11**	A	A	A	A	A	A	–
Classopollis sp. (Fig. 8e)	Coniferales, Cheirolepidiaceae	**8, 11**	r	–	–	r	r	–	–
Cycadopites follicularis	Uncertain affinity	**8**	–	r	r	r	p	p	r
Cycadopites sp. (Fig. 8c)	Uncertain affinity	**8**	r	r	r	p	r	p	A
Equisetosporites spp.	Gnetales, Ephedraceae	**8**	–	–	–	r	r	–	–
Eucommiidites troedsonii	Erdtmanithecales	**8**	–	r	r	r	p	–	p
Eucommiidites cf. *minor* (Fig. 8q)	Erdtmanithecales	**8**	r	–	r	r	r	r	–
Exesipollenites tumulus (Fig. 8p)	Taxodioid? Bennettitales?	**8**	p	R	p	p	C	C	r
Inaperturopollenites dubius (Fig. 8h)	Cupressaceae (Taxodioid?)	**7**	R	R	C	r	A	p	r
Inaperturopollenites spp.	Coniferales (Araucariaceae? Cupressaceae?)	**7, 8**	r	r	p	–	R	r	r
Monosulcites minimus	Uncertain affinity	**6**	–	–	R	r	r	r	–
Monosulcites spp.	Uncertain affinity	**6**	r	r	r	–	r	r	p
Parvisaccites spp. (Fig. 8m, x)	Coniferales, Podocarpaceae	**6**	–	–	r	–	r	r	r
Pinuspollenites spp. (Fig. 8k)	Coniferales, Pinaceae	**6**	r	p	0	r	r	–	r
Podocarpidites sp. (Fig. 8j)	Coniferales, Podocarpaceae	**6**	–	–	–	r	–	–	–
Sciadopityspollenites macroverrucosus	Taxodioid? Sciadopityaceae?	**7**	r	–	–	–	–	–	–
Spheripollenites sp.	Uncertain affinity	Not attributed	p	r	p	r	C	p	R
Steevesipollenites sp. (Fig. 8r–s)	Gnetales, Ephedraceae	**8**	–	–	r	–	r	r	–
Undetermined bisaccate pollen grains	Uncertain affinity (Pinaceae/ Podocarpaceae)	**6**	R	R	–	C	p	r	r
Vitreisporites pallidus	Caytoniales	**7, 10**	r	–	–	–	r	–	–
Pollen grains (angiosperms)									
Clavatipollenites hughesii (Fig. 8n–o)	Chloranthaceae	**2, 5, 9**	–	–	–	–	–	r	r
Crassipollis chaloneri (Fig. 8l)	Uncertain affinity	**5**	–	–	–	r	r	–	–
cf. *Monocolpopollenites* sp. (Fig. 8w)	Arecales, Arecaceae	**6**	–	–	–	r	–	–	–
Retimonocolpites spp. (Fig. 8t–u)	Uncertain affinity	**5**	r	–	r	–	–	–	r
Tucanopollis crisopolensis (Fig. 8v)	Chloranthaceae-*Ceratophyllum* clade	**5, 11**	r	r	r	r	p	r	A

General ecology according to Barrón et al. (2023): 1- Brackish/marine, 2- Freshwater, 3- Marine, 4- Ground cover/xerophytic, 5- Ground cover/hygrophytic, 6- Canopy/xerophytic, 7- Canopy or shrub/xerophytic, 8- Shrub/xerophytic, 9- Pioneer, 10- Coastal, 11-Salt marshes. Semi-quantitative abundances: 1–4 specimens: very rare (r); 5–9 specimens: present (p); 10–19 specimens: rare (R); 20–49 specimens: common (C); > 50 specimens: abundant (A)

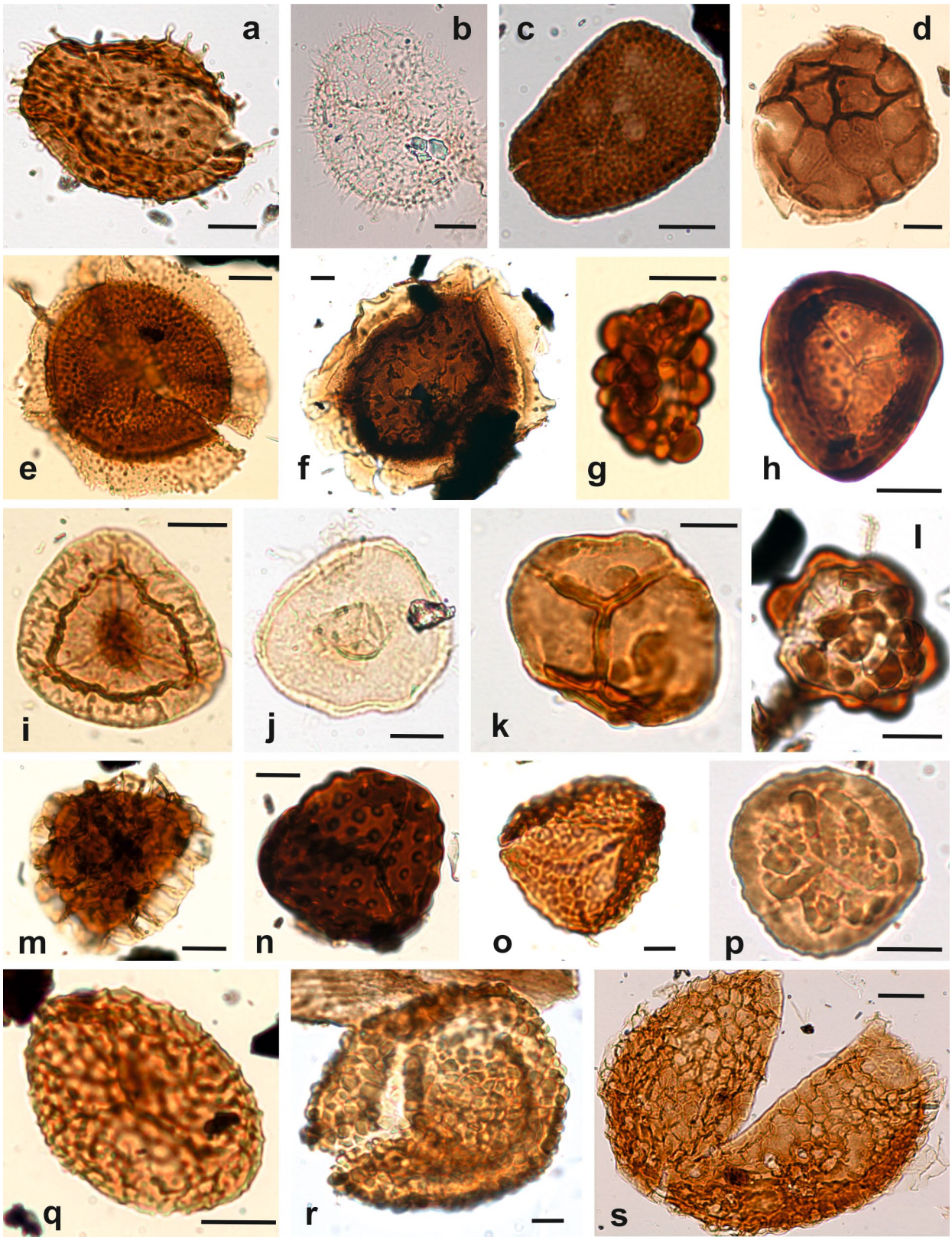
a
b
c
d
e
f
g
h
i
j
k
l
m
n
o
p
q
r
s

◂**Fig. 6** Light photomicrographs of selected marine palynomorphs and bryophytic and lycophytic spores. **a** *Chlamidophorella* sp. (level Po-17). **b** *Cleistosphaeridium* sp. (Ga-3). **c** *Foraminisporis* sp. (Jo-4). **d** *Triporoletes reticulatus* (Po-17). **e** *Aequitriradites verrucosus* (Po-17). **f** *Aequitriradites spinulosus* (Po-15). **g** *Leptolepidites macroverrucosus* (Po-17). **h** *Cingutriletes clavus* (Jo-3). **i** *Staplinisporites telatus* (Po-17). **j** *Stereisporites antiquasporites* (Ga-3). **k** *Stereisporites* sp. (Jo-5). **l** *Leptolepidites proxigranulatus* (Jo-4). **m** *Retitriletes* cf. *facetus* (Jo-3). **n** *Foveosporites* sp. (Po-5). **o** *Foveosporites* cf. *subtriangularis* (Jo-5). **p** *Polycingulatisporites* cf. *reduncus* (focus on the distal side) (Jo-4). **q** *Retitriletes reticulumsporites* (Po-15). **r** *Rubinella major* (Jo-5). **s** *Schizosporis reticulatus* (Jo-5). Graphic scale = 10 µm

of the species *Tucanopollis crisopolensis* (Fig. 8v). All the studied levels are characterized by the scarce presence of aquatic palynomorphs (Fig. 9; Appendix 1), appearing acanthomorph acritarchs, freshwater Zygnemataceae, prasinophytes (Fig. 6s) and poorly preserved marine dinoflagellate cysts. Among the latter, the presence of *Chlamidophorella* sp. and *Cleistosphaeridium* sp. stands out (Fig. 6a, b).

The levels Jo-3 and Jo-4 of the Jorcas section are characterized by the high occurrence of *Classopollis* (mainly *C. obidosensis*), which reached the 46.99% and the 51.71% of abundance, respectively (Fig. 10). In addition, these levels show low but conspicuous percentages of Anemiaceae, mainly *Cicatricosisporites* spp. (Fig. 7c, f–g) and *Araucariacites australis*. Their miospore representation is high considering the diversity of spores (30 and 31 species, respectively) and pollen grains of gymnosperms (16 and 13 species, respectively). Level Jo-4 is relevant by the presence of a single undetermined acanthomorph acritarch and a bad preserved dinocyst (Table 1).

The level Jo-5 from the Jorcas section exhibits higher percentage of spores and lower of pollen of gymnosperms than Jo-3 and Jo-4 (Fig. 10). The abundance of psilate spores of the species *Cyathidites australis* and *Deltoidospora* spp., as well as the occurrence of cf. *Punctatisporites* sp. and *Concavissimisporites informis* (Fig. 7o) is relevant. The percentage of *Classopollis* decreases and is similar of that of *Araucariacites australis* at this level, which also differentiates by the occurrence of the prasinophytes *Pleurozonaria* sp. and *Schizosporis reticulatus* (Fig. 6s). The representation of pollen of angiosperms is very scarce being characterized by the occurrence of *Retimonocolpites* sp. (Fig. 8t, u) at the levels Jo-3 and Jo-5, and *Tucanopollis crisopolensis* at the three levels.

The assemblages of La Porra section show similar features than those of Jo-3 and Jo-4 levels (Fig. 10). The percentage of *Classopollis* pollen grains is higher than 50%. Secondarily, the most representative taxa are *Cicatricosisporites* spp. (Figs. 6r, 7a, b, h) and *A. australis* (Fig. 8b) at the levels Po-15 and Po-17. However, Po-15 differentiates by the percentages of bisaccate pollen grains. The level Po-19 exhibits percentages of *Classopollis* higher than 70%, low diversity of spores (18 species) and conspicuous presence of *Exesipollenites tumulus* (Appendix 1). The levels of La Porra section only show scarce pollen grains of angiosperms of the species *T. crisopolensis*.

The level Ga-3 from the Galve section is very different than those of the Jorcas and La Porra sections because does not present *Classopollis* (Table 1; Fig. 10). The majoritarian palynomorph is *T. crisopolensis* with 58.7% of presence. In addition, this level exhibits the lowest diversity of spores (14 species) being cf. *Punctatisporites* sp. (Fig. 7q) the most usual at this level, and the highest percentages of monosulcate pollen grains that could relate to Cycadales, Bennettitales and Ginkgoales (e.g., *Cycadopites* sp.; Fig. 8c).

4.4 Correspondence analysis

The first correspondence analysis (CA), which included 7 levels and 15 taxa, generated two synthetic dimensions that retained a substantial share of variance (or inertia) of the data set (67% and 23% for dimension I and II, respectively). Based on the study of the absolute and relative contributions of each, a first dimension was defined explaining a gradient of variation with high abundances of angiosperm, mainly *T. crisopolensis*, and monosulcate pollen grains (*Cycadopites/Monosulcites*) at the positive extreme and high abundance of *Classopollis* at the negative one (Fig. 11a). This dimension is finally discriminating the level Ga-3 that has significantly highest abundances of angiosperms and monosulcate pollen grains and a null presence of *Classopollis*. The second dimension is remaking that level Jo-5 has much higher abundance of *Cyathidites/Deltoidospora* than any other level.

Once we know these particularities, we perform a new CA excluding these two levels (Ga-3 and Jo-5) to investigate the common variance of the most similar levels (Fig. 11b). This new CA (5 levels, 15 taxa) generated two new dimensions highly explicative (62% and 27% of inertia, respectively). The first-dimension places levels Po-19 and Po-17 at the positive side and Jo-3, Jo-4 and Po-15 at the negative side. According to the CA results, the most remarkable difference between these two groups of levels is a higher abundance of *Classopollis obidosensis* and lower presence of lycophytic, anemiacean and other producer spores plus the araucariacean and bisaccate pollen in Po-19 and Po-17 (Fig. 10). The second-dimension places Po-17 in the positive side indicating a higher abundance of bryophytic spores and cupressacean (*Inaperturopollenites dubius)* pollen than in the other levels.

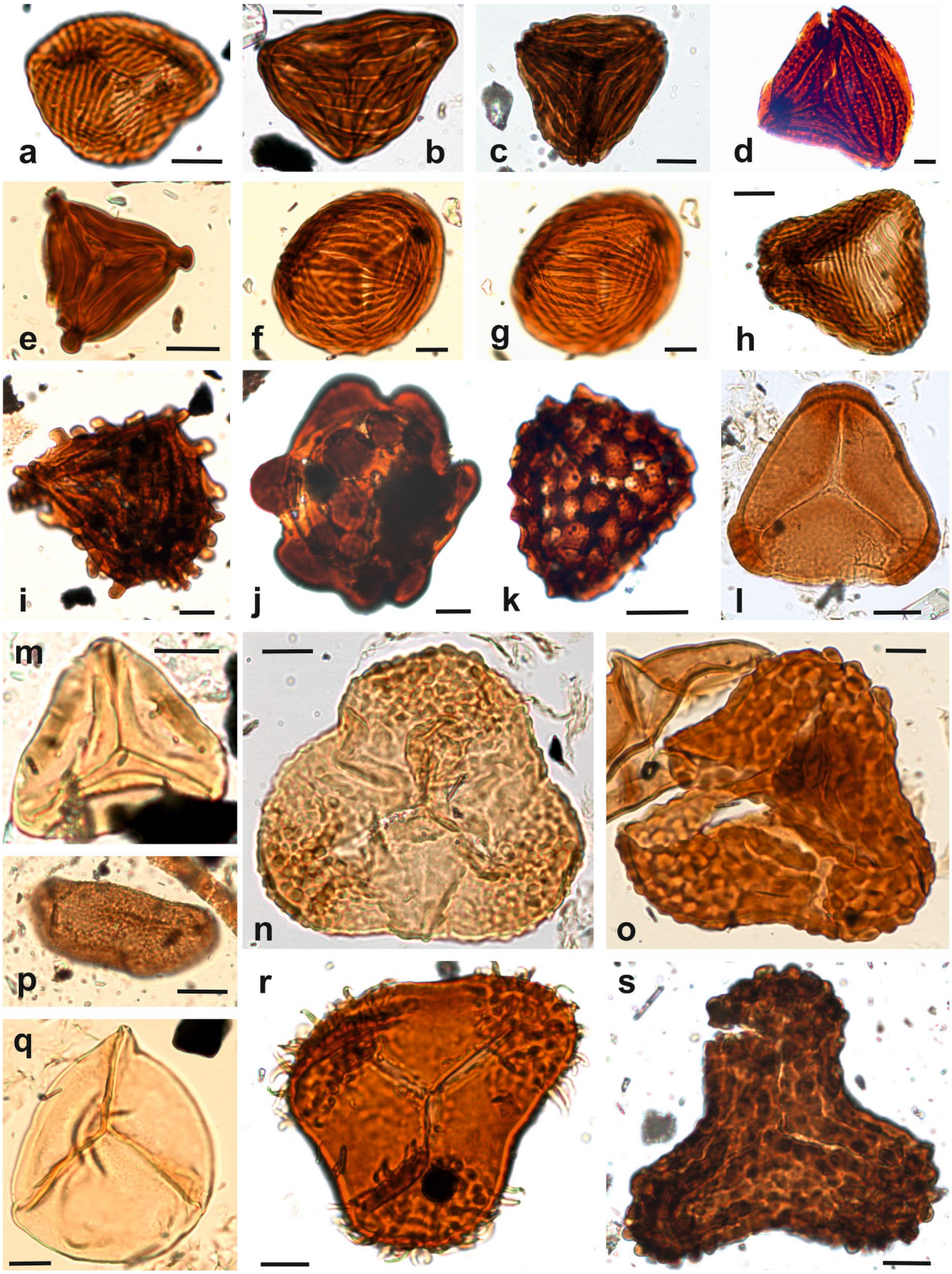
a
b
c
d
e
f
g
h
i
j
k
l
m
n
o
p
r
s
q

◂**Fig. 7** Light photomicrographs of selected fern spores. **a** *Cicatricosisporites venustus* (level Po-15). **b** *Cicatricosisporites* cf. *apicanalis* (Po-17). **c** *Cicatricosisporites* cf. *ludbrookiae* (Jo-3). **d** *Costatoperforosporites* cf. *fistulosus* (Jo-4). **e** *Appendicisporites* sp. (Po-17). **f, g** *Cicatricosisporites potomacensis* (Jo-4): **f** proximal side, **g** distal side. **h** *Cicatricosisporites minutaestriatus* (Po-15). **i** *Nodosisporites* cf. *costatus* (Po-15). **j** *Patellasporites tavaredensis* (Po-15). **k** *Ischyosporites pseudoreticulatus* (Jo-3). **l** *Matonisporites phlebopteroides* (Ga-3). **m** *Gleicheniidites senonicus* (Jo-3). **n** *Trilobosporites purverulentus* (level Ga-3). **o** *Concavissimisporites informis* (level Jo-5). **p** *Verrucatosporites* sp. (Po-19). **q** cf. *Punctatisporites* sp. (Ga-3). **r** *Pilosisporites verus* (Jo-5). **s** *Concavissimisporites apiverrucatus* (Po-19). Graphic scale = 10 µm

5 Discussion

5.1 Palaeoflora age

Although the most of miospore taxa identified in the present paper show long stratigraphic ranges, the studied assemblages indicate a Barremian age. On the one hand, the occurrence of *Cicatricosisporites venustus* (Fig. 7a) in the three sections and *Crassipollis chaloneri* (Fig. 8l) in La Porra section indicates an age not older than the Barremian. Concretely, the oldest records of *C. venustus* come from the Barremian of Maryland (Brenner, 1963) and those of *C. chaloneri* from the Barremian of southeastern Spain (Doubinger & Mas, 1981). On the other hand, the species *Ischyosporites pseudoreticulatus* (Fig. 7k) and *Pilosisporites verus* (Fig. 7r) recognised at Jorcas and La Porra sections have their last occurrences in Spain during the upper Barremian (Leereveld et al., 1989; p. 158).

Considering the angiosperm content of our samples, we have no similarities with the assemblages found in the different zones of the Potomac Group section, which were attributed to the Aptian–early Albian interval (Hochuli et al., 2006). Concretely, the oldest Zone I from the Potomac Group shows more diverse assemblages than the studied ones, characterized by angiosperm species of the genera *Clavatipollenites*, *Liliacidites*, *Pennipollis*, *Stellatopollis* plus *Retimonocolpites* and *Tricolpites* in its upper part (Doyle & Robbins, 1977; Hochuli et al., 2006). On the other, in the well-palynologically known Cocobeach sequence of Gabon (Doyle, 1992; Doyle et al., 1977), the Barremian Zones C-VI and C-VII are also characterized by more diverse angiosperm assemblages with *Clavatipollenites*, *Pennipollis*, *Stellatopollis* and ?*Liliacidites*, although *Tucanopollis crisopolensis* occurs together with the mentioned genera.

In the Iberian Peninsula, the late Barremian assemblages from the Cresmina Formation (Lusitanian Basin, Portugal) only show scarce pollen grains attributable to the genus *Clavatipollenites* (Heimhofer et al., 2007). In addition, although the first occurrence of tricolpate pollen grains in Europe is reported in mid-Barremian strata from the Isle of Wight (Hughes & McDougall, 1990), until now the oldest presence known in the Iberian Peninsula was found in the early Aptian of northern and eastern Spain (Bueno-Cebollada et al., 2021; Najarro et al., 2011). The lack of *Tricolpites* in the studied samples may also be explained by an older age than the Aptian.

In previous works, Pons et al. (2013) recorded in the top of the Camarillas Formation (SE of the Galve village) the angiosperm species *Stellatopollis bituberensis*, *S. hughesi* and *Retimonocolpites* sp. The two first species indicate a Barremian age. Unfortunately, they are not recognised by us in the studied levels. More recently, Villanueva-Amadoz et al. (2015) identified at the Camarillas Formation in the San Cristóbal site (SC-4) the species *Retimonocolpites textus* and *Tucanopollis* sp., and in the Galve Mine site (MG-9) the species *Crassipollis deakae* and *Retimonocolpites* sp. Both palynological sites, prospected at the Galve locality, are located at the middle part of the stratigraphic section of the Camarillas Formation and are associated with vertebrate fossils (Villanueva-Amadoz et al., 2015). These sites are probably included within Stage 2 distinguished for this formation in this work. Except for *C. deakae,* which was described in the Albian of Hungary (Góczán & Juhász, 1984) and recorded with doubt in the late Aptian of Portugal (Trincão, 1990), the rest of pollen grains are compatible with those identified in the studied levels as much for the species recognized as for the low diversity in angiosperm content. Based on the presence of the uninformative species *Cicatricosisporites hughesi*, *Cicatricosisporites hallei* and *Plicatella parviangulata*, Villanueva-Amadoz et al. (2015) also indicate a Barremian age for these two Galve palynological sites.

The Barremian age of the paleoflora is also indicated by the chronological constraints of the Camarillas Formation and the underlying and overlying units (the El Castellar and Artoles formations, respectively). The first biostratigraphic study based on charophytes from the so-called Aliaga Sub-basin was published by Martín-Closas (1989). He found assemblages, which correspond with the *Triquetra-Neimongolensis* Biozone (*Calcitrapus* Subzone) that assigned an early Barremian age to the last part of the Camarillas Formation. However, Navarrete (2015), in her regional study of the Camarillas Formation in the Galve Sub-basin, established that the sediments and charophyte assemblages studied by Martin-Closas (1989) actually form part of the lower part of the Artoles Formation. Riveline et al. (1996) and Aurell et al. (2016) dated the age of the Camarillas Formation as early Barremian—early late Barremian because both the Camarillas and the underlying El Castellar formations comprise the *Atopochara trivolvis triquetra* Zone. Shudack and Shudack (2009) who studied the Lower Cretaceous ostracod assemblages from the Iberian Ranges, dated the Camarillas Formation as early Barremian based on the association of *Cypridea tuberculata, C.* sp. 1,

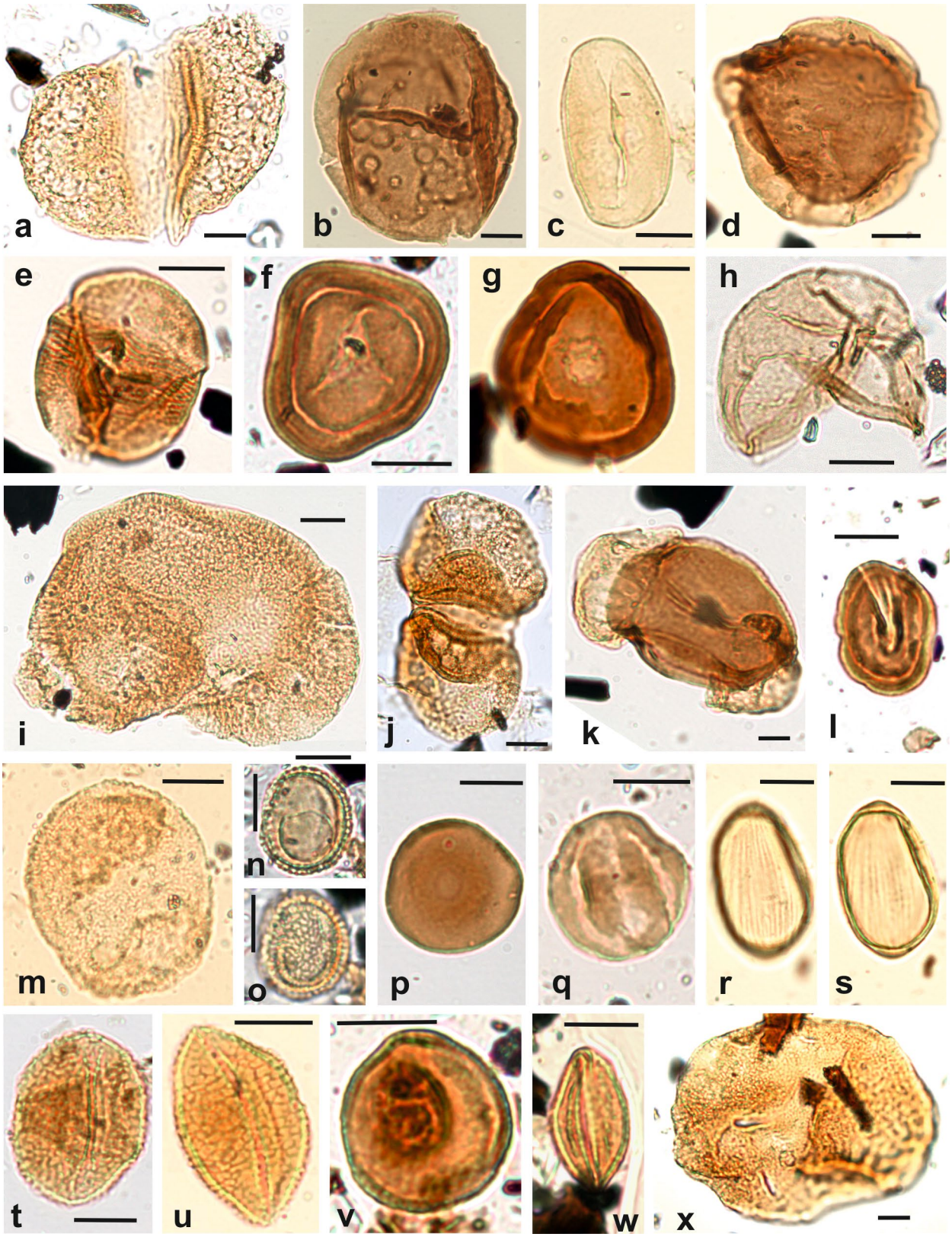
a
b
c
d
e
f
g
h
i
j
k
l
m
n
o
p
q
r
s
t
u
v
w
x

◂**Fig. 8** Light photomicrographs of selected pollen grains of gymnosperms (**a–k, m, p–s, x**) and angiosperms (**n–o, t–w**). **a** *Alisporites bilateralis* (level Ga-3). **b** *Araucariacites australis* (Po-17). **c** *Cycadopites* sp. (Ga-3). **d** *Callialasporites dampieri* (Jo-3). **e** *Classopollis* sp. (Po-15). **f, g** *Classopollis obidosensis*: **f** proximal side with a trilete mark (Po-15), **g** aspect of the distal pore (Jo-3). **h** *Inaperturopollenites dubius* (Jo-3). **i** *Cedripites* cf. *cretaceous* (Ga-3). **j** *Podocarpidites* sp. (Ga-3). **k** *Pinuspollenites* sp. (Jo-5). **l** *Crassipollis chaloneri* (Po-15). **m** *Parvisaccites* sp. (Ga-3). **n, o** *Clavatipollenites* cf. *hughesii* (Po-19): **n** focus on the clavate exine, **o** aspect of the reticulum. **p** *Exesipollenites tumulus* (Jo-5). **q** *Eucommiidites* cf. *minor* (Jo-5). **r, s** *Steevesipollenites* sp. (Po-17): **r** striate ornamentation of the pollen exine, **s** focus on the thickened polar areas. **t, u** *Retimonocolpites* sp. (both Jo-5 level specimens), **v** *Tucanopollis crisopolensis* (Po-17). **w** cf. *Monocolpopollenites* sp. (Po-15). **x** *Parvisaccites* sp. (Jo-4). Graphic scale = 10 µm

C. sp. 2, *C.* sp. C, *Timiriasevia* sp., *Paranotacythere (O.) galvensis, Fabanella Boloniensis, Macrodentina (D.)* aff. *Mediostricta,* and *M. (D.) gibbera.*

Comparing with palynological assemblages of the upper Barremian–Aptian of the Western Desert (Ibrahim, 2002), Pons et al. (2013) attribute the basis of the overhead Artoles Formation in the Galve Sub-basin, to the late Barremian from an inconclusive assemblage with aff. *Arecipites microfoveolatus*, *Afropollis* sp., *Stellatopollis barghoornii*, fresh water palynomorphs and dinocysts. A late Barremian–early Aptian age for this formation was also attributed mainly from the charophyte associations (Canudo et al., 1996; Salas et al., 1995). The age of the Artoles Formation in the Galve Sub-basin has recently been constrained to the Barremian based on palinological data, specifically by the presence of *Pilosisporites trichopapillosus*, *P. verus*, *Callialasporites trilobatus*, *Aequitriradites spinulosus* and *Stellatopollis bituberensis*, and to the late Barremian from nannoplankton biostratigraphy (first appearance of *Rhagodiscus amplus*) (Lopes, 2018).

In summary, the Barremian age indicated by palynological data of the Camarillas Formation may be constrained to the early to the early late Barremian if palynological assemblages are considered together with the charophyte and ostracod data (Martín-Closas, 1989; Schudack & Schudack, 2009). This age is also supported by the biostratigraphy of ostracod, charophyte and palynological assemblages of the underlying El Castellar Formation (Badiola et al., 2011; Canudo et al., 2012; Gasca, 2015; Martín-Closas, 1989; Soria, 1997) and that of these assemblages and of nannoplankton from the overlying Artoles Formation (Lopes, 2018; Martín-Closas, 1989; Schudack & Schudack, 2009).

5.2 Palaeovegetation and paleoenvironments

The reconstructions of Mesozoic environments based on palynological studies are complex, since many plants that existed during this Era usually have no modern counterparts and this generally prevents actualistic studies from being undertaken. The marine influence of the studied samples is well indicated by the presence of dinoflagellate cysts in most of the studied levels (Jo-4, Jo-5, Po-17, Po-19 and Ga-3) and, particularly by the occurrence of *Cleistosphaeridium* sp. and *Chlamidophorella* sp. These results align with sedimentological interpretations as productive samples from the Jorcas and La Porra sections were collected from the central bay muds, back-barrier tidal mud flats and tidal channel (intertidal zone) facies (Figs. 2, 3) associated with the outer and inner parts of the mixed tide- and wave-dominated estuary (Soria et al., 2023). They characterize the Stage 2 of the sedimentary evolution of the Camarillas Formation (Fig. 5), whose assemblages are mainly integrated by miospores (Figs. 9, 10).

According to Courtinat et al. (2002), terrestrial components recovered from marine depositional sequences are usually numerically dominated by miospores produced by coastal and regional vegetation. In the case of the studied levels, the unsubstancial presence of acritarchs and dinoflagellate cysts suggests a proximal setting characterized by a weak marine influence, which is in clear accordance with the palaeogeographic interpretation of the Camarillas Formation (Fig. 1d) proposed by Soria et al. (2023). Specificallly, the palynological assemblages inferred in the Jorcas and La Porra sections occur in sediments deposited in a tide- and wave-dominated estuary. They are probably the result of the accumulation of miospores transported by water currents and wind, so they may be partially biased. Except for the level Jo-5, the assemblages of the Jorcas and La Porra sections present similar percentages of palynomorphs (Fig. 10). The main difference is a progressive increase of *Classopollis* and a decrease of the rest of miospore groups in the La Porra section. These values may be related to an increased input of *Classopollis* transported by water streams or to changes in vegetation that favoured the spread of its producing plants.

Classopollis (Fig. 8e–g), which is the most abundant palynomorph in the Camarillas Formation, was produced by extinct voltzialean conifers of the Cheirolepidiaceae family (Jarzen & Nichols, 1996), one of the most widespread conifer families among the Mesozoic vegetation. While historically linked to arid environments and/or salty ones (Hotton & Baghai-Riding, 2010; Watson, 1988), recent studies suggest broader ecological preferences for, at least, some representatives of the family (Tosolini et al., 2015). Some species of this family lived in coastal and saline environments (Alvin, 1982; Watson, 1988), which is in

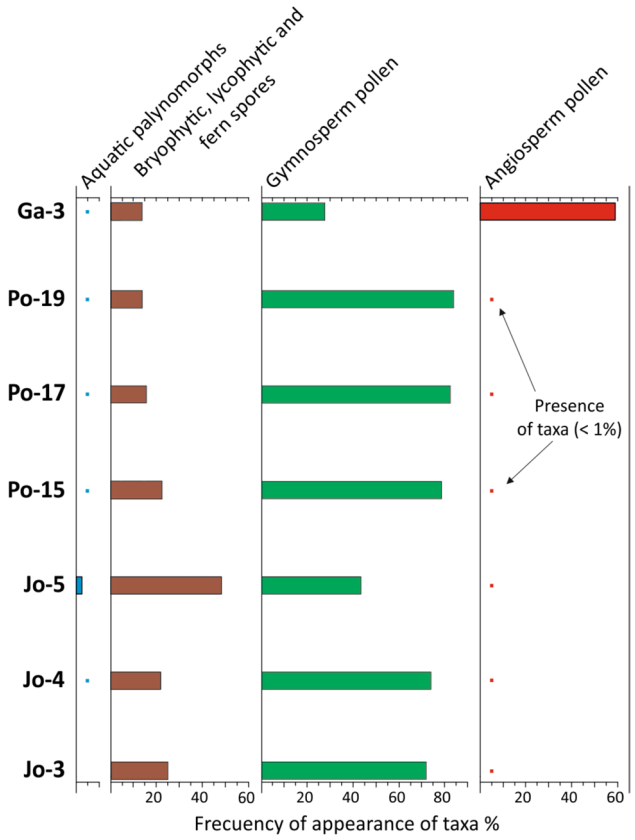

Fig. 9 Pollen diagram showing the abundances as percentages per level of the main identified groups of palynomorphs

agreement with the palaeoenvironmental reconstructions proposed for the Camarillas Formation (e.g., Navarrete et al., 2013b, 2014). The importance of Cheirolepidiaceae in the Barremian of Galve was previously manifested by Mohr (1987, 1989) and Villanueva-Amadoz et al. (2015) from the high representation of *Classopollis* as well as the occurrence of macroremains of the species *Pseudofrenelopsis* aff. *varians*. Possibly, the representatives of Cheirolepidiaceae from the Camarillas Formation were shrub and/or trees that grew forming thickets in stressed places near the Tethyan coasts.

After *Classopollis*, bryophytic and pteridophytic spores are the most abundant palynomorphs. In addition, they are the most biodiverse (67 species; Table 1). Although dispersion by wind have been reported in a certain number of cases in spores of pteridophytes (Ferguson & Knobloch, 1998), they remain strongly reliant on water. The spores are generally heavier than pollen grains and they accumulate close to the ferns that produce them (leptokurtic distribution, sensu Ferguson [1995]). Possibly, the conspicuous spore percentages in all studied levels mainly relate to the parautochthony of the inferred assemblages. Generally, the most producers of the species identified were hygrophytic and grew on lowlands, in riparian places or/and in the understory of coniferous forest (Table 1). By their abundance, the spore species *Cicatricosisporites* spp., *Cyathidites australis*, *Deltoidospora* sp. and cf. *Punctatisporites* sp. are relevant in the studied levels (Fig. 10; Table 1). The existence of swampy and/or lacustrine environments with permanent or semi-permanent water level in the Galve Sub-basin and its surroundings during the Barremian is confirmed by the occurrence of spores that needed high moisture to reproduce.

The occurrence with low percentages of Araucariaceae pollen grains is interesting (Fig. 10). This family produced wind-dispersed inaperturate pollen. However, the presence and relative abundance of these conifers in the local vegetation may be underestimated since both modern (Caccavari, 2003; Elliot, 1999; Sousa & Hattemer, 2003) and fossil Araucariacean pollen (Peyrot et al., 2019) are believed to present low pollen dispersal capabilities, also indicating leptokurtic distribution. Its values may be related to trees that grew near seashores (Abbink et al., 2004) such as some recent species, such as *Araucaria columnaris*, *A. luxurians* and *A. nemorosa* (Pillon, 2012).

Conifers producing bisaccate pollen grains, such as Pinaceae and Podocarpaceae (Fig. 8a, i–k, m, x; Fig. 10), are poorly represented in the studied levels. Comparing with their extant relatives, if these families had been common in the zone their pollen grains would occur over-represented, since bisaccate grains are generally abundantly produced and they are long-distance transported by winds and/or waters (Traverse, 2007). Their low percentages could indicate that these plants grew on uplands far away the zone of fossilization.

The level Jo-5 exhibits an interesting assemblage with remarkable percentages of spores (cf. *Punctatisporites* sp., *Cyathidites australis*, *Deltoidospora* sp.) and pollen of *Araucariacites australis*, *Inaperturopollenites dubius* and *Monosulcites minimus*, as well as the decrease of *Classopollis* with a 13% of presence (Fig. 10). The different palynological signature of this assemblage is also indicated by the first correspondence analysis (Fig. 11a). It seems to be related to a relevant influence of continental swampy or lacustrine influence indicating an increase of moisture in the environment. Levels Jo-4 and Jo-5 were collected in a back-barrier mud flat facies of the outer part of the estuary; in particular Jo-5 corresponds to supratidal claystones showing pedogenic features. The picture of the vegetation may be a riparian forest of gymnosperms with Cupressaceae (taxodioids) and *Cycadopites/Monosulcites*-producers (cycas, ginkgos or/and Bennettitales) with an undergrown of ferns with scarce angiosperms. Out of this plant community, Cheirolepidiacean thickets developed in drier places and Araucariacean woods dominated in coastal areas. The assemblages of the Jorcas section show resemblances with these from the Barremian from Villar del Arzobispo (East

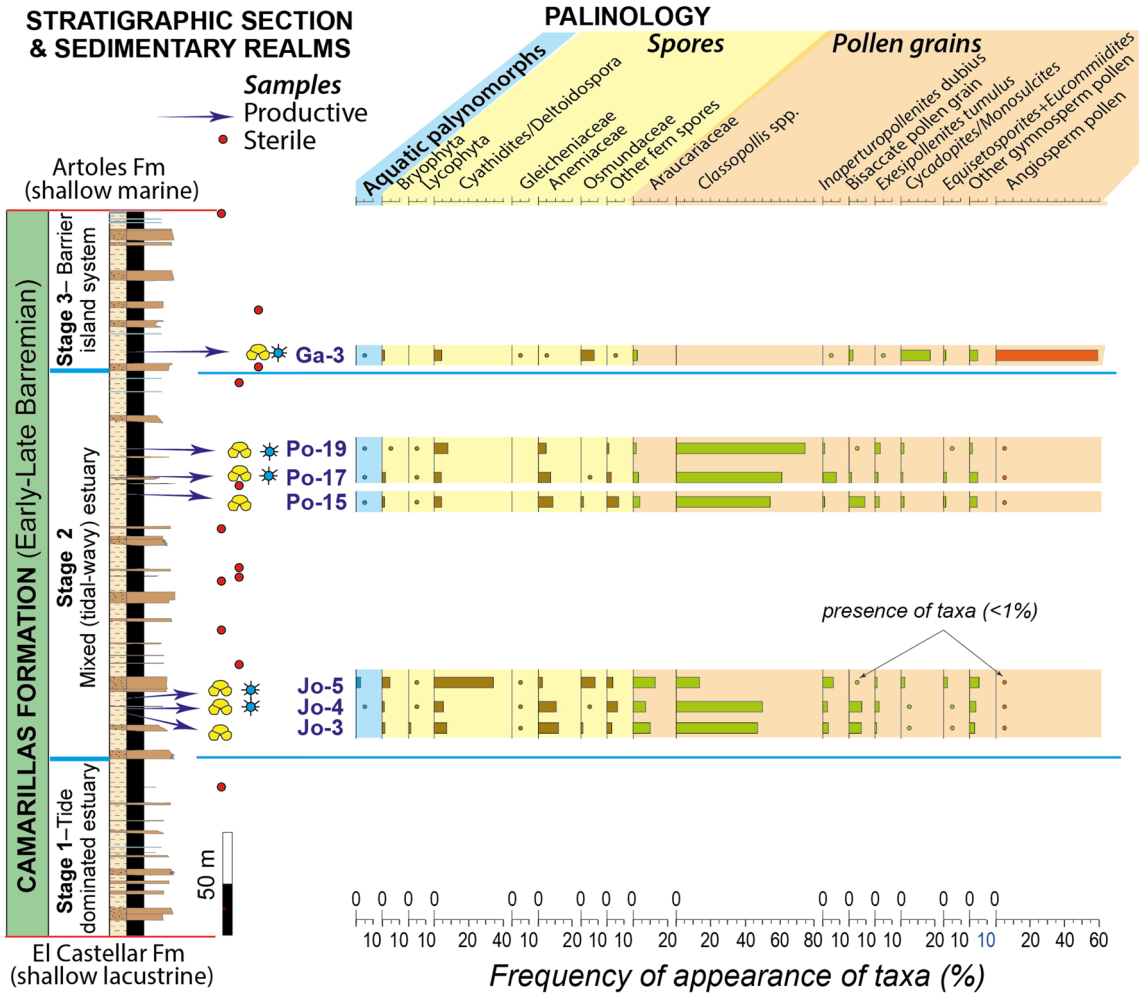

Fig. 10 Synthetic stratigraphic section of the Camarillas Formation with the location of the productive and sterile samples, and pollen diagram showing the variations in identified taxa and their relative percentages throughout the succession. The botanical affinities of these taxa, general ecology and abundance of each one can be found in Table 1 and Appendix 1

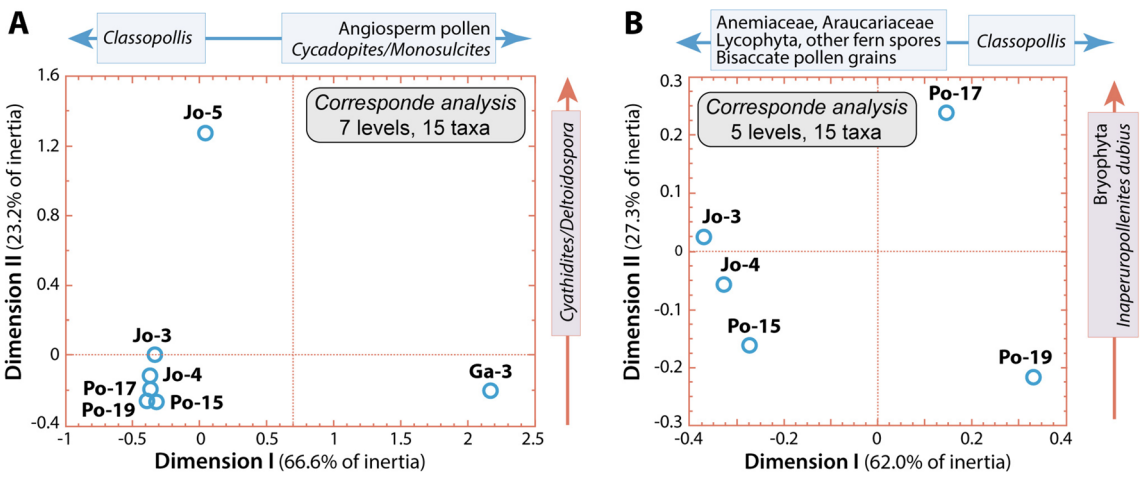

Fig. 11 Correspondence analysis (CA) result. **a** CA diagram performed with the complete data matrix (7 levels and 15 taxa). **b** CA diagram after extracting Ga-3 and Jo-5 (5 levels and 15 taxa). The taxa placed at the extremes of each dimension are those that have contributed the most to the constitution of each dimension

Spain) (Doubinger & Mas, 1981) due to the percentages of spores (44%) and *Classopollis* (51%) that exhibit.

The occurrence of the angiosperm pollen *Tucanopollis crisopolensis* (Fig. 8v) is relevant in the Ga-3 level (Table 1). This species was reported in the Barremian to the early Aptian in Brazil and west and north-east Africa (Doyle et al., 1977; Herngreen et al., 1996; Regali, 1989; Regali et al., 1974). In addition, *T.* cf. *crisopolensis* has been found in early Albian sediments from Brazil (Heimhofer & Hochuli, 2010), *T.* aff. *crisopolensis* in lower Aptian and lower Albian materials of the Algarve Basin, Portugal (Heimhofer et al., 2007) and *T. crisopolensis* in late Albian of the Basque-Cantabrian and the Maestrazgo basins (Barrón et al., 2015, 2023). Pollen similar to *Tucanopollis* occurred linking with fruits of *Appomattoxia* in late Barremian–early Aptian of Portugal and early–middle Albian of Virginia (Friis et al., 2011). Moreover, it has been observed in stamens of the angiosperm *Pseudoasterophyllites cretaceous*, which lived in salt marsh habitats of the Albian and Cenomanian of Europe (Kvaček et al., 2012, 2016). The relevant presence of this pollen in Ga-3 may indicate the existence of xerophytic vegetation integrated by grooves of *Cycadopites/Monosulcites*-producers in dry areas, riparian formations with ferns (*Cyathidites* and cf. *Punctatisporites* sp. producers) and semi-aquatic/pioneer vegetation integrated by angiosperms (mainly *Tucanopollis*-producer) in possibly halophytic marshes. This is consitent with the location of the level (Fig. 4), which was taken in sediments that has been interpreted as deposited within a marsh developed on the tidal flat within a lagoon protected by a barrier island system (Navarrete, 2015; Soria et al., 2023).

Tucanopollis had during the Early Cretaceous a majoritarian Gondwanan distribution, although its records in South Europe classified it as "an angiosperm pollen with a semi-restricted distribution" (Boukhamsin et al., 2022). A level with high values of *Tucanopollis* was also identified in the late Albian of the Cortes de Arenoso succession in the Maestrazgo Basin also indicating halophytic/xerophytic vegetation (Barrón et al., 2023).

The palynoflora of the Camarillas Formation clearly distinguishes itself from that of the Barremian of Portugal by its low abundance and diversity of dinoflagellate cysts. The notable presence of dinocysts in Portugal is associated with the influence of Atlantic waters (Heimhofer et al., 2007; Mendes et al., 2023). Similar to the Camarillas Formation, the Portuguese Barremian miospore assemblages are also composed of spores and pollen grains. Gymnosperm pollen, although less diverse than spores, consistently predominates, with *Classopollis*, *Araucariacites*, *Callialasporites* and some bisaccates being the most relevant. Spores are mainly represented by diverse taxa such as *Concavissimisporites*, *Cyathidites*, *Foveosporites*, *Gleicheniidites*, *Patellasporites*, *Staplinisporites*, *Trilobosporites* and Anemiaceae (Pais & Reyre, 1980–1981; Taugourdeau-Lantz, 1988; Leereveld et al., 1989; Mendes et al., 2023), which are also found in the Camarillas Formation. In contrast, Portuguese angiosperm pollen is only represented by *Clavatipollenites* as pollen dispersae (Heimhofer et al., 2005, 2007) and by *Clavatipollenites* and *Pennipollis* in floral mesofossils (Friis et al., 2000, 2011). On the other hand, the late Barremian–early Aptian dating of the Casal do Borracho outcrop as (Mendes et al., 2018) should be revised due to the occurrence of Albian–Cenomanian spores, such as *Crybelosporites pannuceus*, within its assemblage. Alternatively, the appearance of this specific taxon itself may require re-evaluation.

In summary, the flora that developed in the Galve Sub-basin during the deposit of the Camarillas Formation was characterized by the existence of mosaic vegetation types with conifer-forests along the Tethyan coasts. More concretely, it was determined by (i) arid places with woodlands of Cheirolepidiaceae, (ii) coastal forests of Araucariaceae, (iii) freshwater swamps with taxodioids and ferns, and (iv) brackish swamps with angiosperms and *Cycadopites/Monosulcites*-producers. This vegetation is mainly related to the Mesophytic floras in the sense of Traverse (2007), due to the dominant gymnosperm pollen and the high diversity of bryophytic and fern spores indicating highly diversified spore-producing plants communities.

5.3 Evolutionary trends

The 63% of the analyzed samples resulted to be barren of palynomofs (Fig. 10). This has happened independently of the lithofacies analyzed; 100% of the samples are black to gray organic matter-rich levels, which were interpreted by Navarrete (2015) and Soria et al. (2023) as corresponding mainly to central bay muds and clay tidal flats with marshes developed in an estuary and lagoon facies (Figs. 2, 3, 4). There is no evident reason why similar lithofacies should provide a percentage as high as the 63 of barren samples. It has been suggested that oxidation is the main factor causing palynological sterility, as well as washing, wet-dry cycles, cementation or bioturbation, among others (Carrión et al., 2009). However, none of these processes have been recognized during field campaigns at the levels sampled for palynological analysis; again, productive and sterile lithofacies are the same but yielded completely different palynomorph contents. A palyno-taphonomic approach to this problem has not been possible either. The miospores in productive samples are very well preserved (Figs. 6, 7, 8) and the other samples have no palynological content, so poorly preserved palynomorphs have not been found either.

Despite being a discontinuous palynological record, the productive samples show that the mosaic vegetation

was not always the same throughout the stratigraphic sucession and, therefore, over time. As the pollen diagram of the Jorcas and La Porra samples (Stage 2) suggests, woodlands of Cheirolepidiaceae and the coastal forests of Araucariaceae are in competition and evolve inversely against each other, so that when one decreases the another increases and vice versa (Fig. 10). Specifically, *Classopollis* decreases slightly upward in the succession in the Jorcas levels and then increases upward in the La Porra section levels, while Arauricariacean pollen shows the opposite trend. Correspondence analysis (CA) also shows how Araucariacean pollen varies inversely to that of *Classopollis* (Fig. 11a). Furthermore, the second CA indicates that Araucariaceae characterizes a different level group than Cheirolepidiaceae (Fig. 11b). Thus, we could speculate that how Araucariaceae became linked to Cheirolepidiaceae (*Classopollis* spp.) during the deposition of the Camarillas Formation, being recorded at the same stratigraphic levels, the trend shown by these pollen grains (Fig. 10) probably represents an evolving environmental landscape. This evolution of the paleoflora landscape could be related to long- or short-term variations in environmental factors, perharps due to palaeoclimate changes of astronomical origin (e.g., Illueca et al., 2024). In any case, the poor temporal adjustment of the stratigraphic series, the stratigraphic/time separation between the Jorcas and La Porra levels, as well as the high number of sterile samples existing in between, prevents a deeper analysis of these environmental changes and their control and modulation factors.

Finally, the beginning of the Stage 3 (Ga-3) shows an abrupt change with the previous paleoflora of Stage 2. The pollen of Araucariaceae and Cheirolepidiaceae practically disappear and the palaeoflora is mainly characterized by salt-tolerant semi-aquatic angiosperms and *Cycadopites*/*Monosulcites*-producers. This palaeoflora, especially angiosperms, is typical of brackish marshes, which agrees, as indicated, with the sedimentological interpretation of Navarrete (2015) and Soria et al. (2023) of the host sediments (Fig. 4). Consequently, angiosperms may represent in situ palaeoflora, that is, they developed within the sedimentary environment where sediment deposition took place.

In sumamry, although the palaeoflora record is highly discontinuous in the Camarillas Formation, the results suggest that plant ecosystems evolved over time. The variations in the plant ecosystem could be associated with environmental and palaeoclimatic changes that occurred during the Barremian in western Tethys. On the other hand, more research is needed to evaluate the value of the negative results of palynological studies. They are only the expression of the post-depositional destruction of the palynological content of the sediments or, on the contrary, they may indicate periods of very poor development of palynological producers and/or a very limited areal distribution of miospores from forests and open-lands developed in surrounding continental areas, so they do not reach the sedimentation basin.

6 Summary

The palynological study of the Camarillas Formation (Early Cretaceous), Galve Sub-basin, has confirmed its Barremian age and provided new palaeoenvironmental and palaeoclimatic insights into the evolution of coastal ecosystems in the Western Tethys. The presence of bad preserved dinoflagellate cysts indicates the marine influence in the studied samples. The information obtained from the palynological study suggests plant ecosystems characterized by coastal coniferous forest. The occurrence of *Tucanopollis crisopolensis* related the studied flora with the North of Gondwana province and with semi-aquatic salt-tolerant angiosperms which reflect a restricted marshy environment. The palynological record is highly discontinuous due mainly to the high number of sterile samples, although they were collected in very similar sedimentary facies, that is, black to gray mud levels rich in organic matter from a protected estuary or lagoon (mud from the central bay or from marshes in tidal mudflats). Furthermore, the palynological record shows palaeovegetation and palaeoenvironment that evolved over time.

Supplementary Information The online version contains supplementary material available at https://doi.org/10.1007/s41513-025-00299-5.

Acknowledgements This paper is dedicated to Professor Antonio Goy, who teach Palaeontology at the UCM during more than forty years. Although he mainly devoted himself to the study of the Early Jurassic ammonoids during his professional career, he was also interested in different fossil groups such as the Mesozoic palynomorphs. This work is a contribution to the study of the Spanish Cretaceous, to which he also spent part of his scientific activity. We wish to acknowledge to the ALI-CONTROL laboratory (Madrid, Spain) and Manuel Casas Gallego for samples preparation, Daniel Peyrot (MGpalaeo, Western Australia) for his aid in the identification of the dinocysts from the Camarillas Formation, the Servicio General de Apoyo a la Investigación-SAI from the Zaragoza University (Spain) and the two anonymous referees who provided valuable suggestions for the improvement of the manuscript. This research has been carried out within the Research Projects DISCLI-TECT (Grant PID2019-108705-GB-I00), CREI (PID2022-137316NB-C22) and IBERCRET (PID2023-148949NB-I00) funded by MICIU/AEI/https://doi.org/10.13039/501100011033 and by ERDF/EU, and the GEOtransfer Research Group (Grant E32_23R) funded by the Aragón Government (Spain).

Funding Open Access funding provided thanks to the CRUE-CSIC agreement with Springer Nature.

Declarations

Conflict of interest On behalf of all authors, the corresponding author states that there is no conflict of interest.

References

Abbink, O. A., Van Konijnenburg-Van Cittert, J. H. A., & Visscher, H. (2004). A sporomorh ecogroup model for the Northwest European Jurassic – Lower Cretaceous: Concepts and framework. *Geologie en Mijnbouw, 83*(1), 17–38. https://doi.org/10.1017/S0016774600020436

Álvaro, M., Capote, R., & Vegas, R. (1979). Un modelo de evolución geotectónica para la Cadena Celtibérica. *Acta Geológica Hispánica, 14*, 172–177.

Alvin, K. L. (1982). Cheirolepidiaceae: Biology, structure and palaeoecology. *Review of Palaeobotany and Palynology, 37*, 71–98. https://doi.org/10.1016/0034-6667(82)90038-0

Antolín-Tomas, B., Liesa, C. L., Casas, A. M., & Gil-Peña, I. (2007). Geometry of fracturing linked to extensión and basin formation in the Maestrazgo Basin (Eastern Iberian Chain, Spain). *Revista de la Sociedad Geológica de España, 20*(3–4), 351–365.

Aurell, M., Bádenas, B., Gasca, J. M., Canudo, J. I., Liesa, C., Soria, A. R., Moreno-Azanza, M., & Najes, L. (2016). Stratigraphy and evolution of the Galve sub-basin (Spain) in the middle Tithonian–early Barremian: Implications for the setting and age of some dinosaur fossil sites. *Cretaceous Research, 65*, 138–162. https://doi.org/10.1016/j.cretres.2016.04.020

Aurell, M., Fregenal-Martínez, M., Bádenas, B., Muñoz-García, M. B., Élez, J., Meléndez, N., & de Santisteban, C. (2019). Middle Jurassic—Early Cretaceous tectono-sedimentary evolution of the southwestern Iberian Basin (central Spain): Major palaeogeographical changes in the tectonic framework of the Western Tethys. *Earth Science Reviews, 199*, 102983. https://doi.org/10.1016/j.earscirev.2019.102983

Badiola, A., Canudo, J. I., & Cuenca-Bescós, G. (2011). A systematic reassessment of Early Cretaceous multituberculates from Galve (Teruel, Spain). *Cretaceous Research, 32*, 45–57. https://doi.org/10.1016/j.cretres.2010.10.003

Barrón, E., Peyrot, D., Bueno-Cebollada, C. A., Kvaček, J., Álvarez-Parra, S., Altolaguirre, Y., & Meléndez, N. (2023). Biodiversity of ecosystems in an arid setting: The late Albian plant communities and associated biota from eastern Iberia. *PLoS ONE, 18*(3), Article e0282178. https://doi.org/10.1371/journal.pone.0282178

Barrón, E., Peyrot, D., Rodríguez-López, J. P., Meléndez, N., López del Valle, R., Najarro, M., Rosales, I., & Comas-Rengifo, M. J. (2015). Palynology of Aptian and upper Albian (Lower Cretaceous) amber-bearing outcrops of the southern margin of the Basque-Cantabrian basin (northern Spain). *Cretaceous Research, 52*, 292–312. https://doi.org/10.1016/j.cretres.2014.10.003

Barrón, E., Ureta, S., Goy, A., & Lassaletta, L. (2010). Palynology of the Toarcian-Aalenian Global Boundary Stratotype Section and Point (GSSP) at Fuentelsaz (Lower–Middle Jurassic, Iberian Range, Spain). *Review of Palaeobotany and Palynology, 162*(1), 11–28. https://doi.org/10.1016/j.revpalbo.2010.04.003

Batten, D. J. (1999). Small palynomorphs. In T. P. Jones & N. P. Rowe (Eds.), *Fossil plants and spores: Modern techniques* (pp. 15–19). The Geological Society of London.

Benzécri, J. P. (1973). *L'analyse des Données, vol. 2. L'analyse des correspondances*. Dunod, Paris.

Blackey, R. (2014). http://cpgeosystems.com/125_Cret_EurMap_sm.jpg

Boukhamsin, H., Peyrot, D., & Vecoli, M. (2022). Angiosperm pollen assemblages from the Lower Cretaceous (Barremian—lower Aptian) of offshore Saudi Arabia and their implications for early patterns of angiosperm radiation. *Palaeogeography, Palaeoclimatology, Palaeoecology, 599*, Article 111052. https://doi.org/10.1016/j.palaeo.2022.111052

Bover-Arnal, T. (2010). *The Aptian evolution of the Galve Sub-basin (Maestrat Basin, E Iberia).* Ph.D. thesis, University of Bayreuth. http://opus.ub.uni-bayreuth.de/volltexte/2010/671

Brenner, G. J. (1963). The spores and pollen of the Potomac Group of Maryland. *Maryland Department of Geology, Mines and Water Research Bulletin, 27*, 1–215.

Bueno-Cebollada, C. A., Barrón, E., Peyrot, D., & Meléndez, N. (2021). Palynostratigraphy and palaeoenvironmental evolution of the Aptian to lower Cenomanian succession in the Serranía de Cuenca (Eastern Spain). *Cretaceous Research, 128*, Article 104956. https://doi.org/10.1016/j.cretres.2021.104956

Caccavari, M. (2003). Dispersión del polen en *Araucaria angustifolia* (Bert.) O. Kuntze. *Revista del Museo Argentino de Ciencias Naturales, 5*(2), 135–138.

Canudo, J. I., & Cuenca-Bescós, G. (1996). Two new mammalian teeth (Multituberculata and Peramura) from the Lower Cretaceous (Barremian) of Spain. *Cretaceous Research, 17*, 215–218. https://doi.org/10.1006/cres.1996.0016

Canudo, J. I., Cuenca-Bescós, G., Ruiz-Omeñaca, J. I., & Soria, A. R. (1996). Estratigrafía y paleoecología de los vertebrados del Barremiense superior (Cretácico Inferior) de Vallipón (Castellote, Teruel). *Mas De Las Matas, 15*, 9–34.

Canudo, J. I., Gasca, J. M., Moreno-Azanza, M., & Aurell, M. (2012). New information about the stratigraphic position and age of the sauropod *Aragosaurus ischiaticus* from the Early Cretaceous of the Iberian Peninsula. *Geological Magazine, 149*, 252–263. https://doi.org/10.1017/S0016756811000732

Capote, R., Muñoz, J. A., Simón, J. L., Liesa, C. L., & Arlegui, L. E. (2002). Alpine tectonics I: The Alpine system north of the Betic Cordillera. In W. Gibbons & T. Moreno (Eds.), *Geology of Spain* (pp. 367–400). The Geological Society of London.

Carrión, J. S., Fernández, S., González-Sampériz, P., Leroy, S. A. G., Bailey, G. N., López-Sáez, J. A., Burjachs, F., Gil-Romera, G., García-Antón, M., Gil-García, M. J., Parra, I., Santos, L., López-García, P., Yll, E. I., & Dupré, M. (2009). Quaternary pollen analysis in the Iberian Peninsula: The value of negative results. *Internet Archaeology, 25*, 1–51.

Courtinat, B., Rio, M., & Malartre, F. (2002). Palynofacies of marginal deposits: The Rhaetian of the east margin of the Massif Central (France). *Revue De Micropaléontologie, 45*(1), 47–55. https://doi.org/10.1016/S0035-1598(02)80005-8

Davis, R. A., Yale, K. E., Pekala, J. M., & Hamilton, M. V. (2003). Barrier island stratigraphy and Holocene history of west-central Florida. *Marine Geology, 200*, 103–123. https://doi.org/10.1016/S0025-3227(03)00179-8

De la Fuente, M., & Zetter, R. (2016). Palynomorphs. In F. J. Poyato-Ariza & A. D. Buscalioni (Eds.), *Las Hoyas: A Cretaceous wetland* (pp. 31–42). Verlag Dr. Friedrich Pfeil.

Díaz Molina, M., & Yébenes, A. (1987). La sedimentación litoral y continental durante el Cretácico Inferior, sinclinal de Galve, Teruel. *Estudios Geológicos*, *vol. extraord. Galve-Tremp*, 3–21. https://doi.org/10.3989/egeol.8743Extra623

Diéguez, C., Peyrot, D., & Barrón, E. (2010). Floristic and vegetationsl changes in the Iberian Peninsula during Jurassic and Cretaceous. *Review of Palaeobotany and Palynology, 162*, 325–340. https://doi.org/10.1016/j.revpalbo.2010.06.004

Doubinger, J., & Mas, J. R. (1981). Une microflore du Barrémien dans la province de Valencia, Espagne. *Cretaceous Research, 2*, 51–64. https://doi.org/10.1016/S0195-6671(81)80004-3

Doyle, J. A. (1992). Revised palynological correlations of the lower Potomac Group (USA) and the Cocobeach sequence of Gabon (Barremian—Aptian). *Cretaceous Research, 13*, 337–349. https://doi.org/10.1016/0195-6671(92)90039-S

Doyle, J. A., Biens, P., Doerenkamp, A., & Jardiné, S. (1977). Angiosperm pollen from the pre-Albian Lower Cretaceous of equatorial Africa. *Bulletin des Centres De Recherche De Exploration-Production Elf-Aquitaine, 1*(2), 451–473.

Doyle, J. A., & Robbins, E. I. (1977). Angiosperm pollen zonation of the Continental Cretaceous of the Atlantic Coastal Plain and its application to deep wells in the Salisbury embayment. *Palynology, 1*, 43–78. https://doi.org/10.1080/01916122.1977.9989150

Elliot, M. B. (1999). Modern pollen–vegetation relationships in Northland, New Zealand. *New Zealand Journal of Botany, 37*, 131–148. https://doi.org/10.1080/0028825X.1999.9512619

Ferguson, D. K. (1995). Plant part processing and community reconstruction. *Eclogae Geologie Helveticae, 88*(3), 627–641.

Ferguson, D. K., & Knobloch, E. (1998). A fresh look at the rich assemblage from the Pliocene sink-hole of Willershausen, Germany. *Review of Palaeobotany and Palynology, 101*, 271–286. https://doi.org/10.1016/S0034-6667(97)00078-X

Friis, E. M., Crane, P. R., & Pedersen, K. R. (2011). *Early flowers and angiosperm evolution*. Cambridge University Press.

Friis, E. M., Grimm, G. W., Mendes, M. M., & Pedersen, K. R. (2015). *Canrightiopsis*, a new Early Cretaceous fossil with *Clavatipollenites*-type pollen bridge the gap between extinct *Canrightia* and extant Chloranthaceae. *Grana, 54*(3), 184–212. https://doi.org/10.1080/00173134.2015.1060750

Friis, E. M., Pedersen, K. R., & Crane, P. R. (2000). Fossil floral structures of a basal angiosperm with monocolpate, reticulate-acolumellate pollen from the Early Cretaceous of Portugal. *Grana, 39*, 226–239. https://doi.org/10.1080/00173130052017262

Gale, A. S., Mutterlose, J., Battenburg, S., Gradstein, F. M., Agterberg, J. G., Ogg, J. G., & Petrizzo, M. R. (2020). The Cretaceous Period. In F. M. Gradstein, J. G. Ogg, M. D Schmitz & G. M. Ogg (Eds.), *The Geological Time Scale 2020* (Vol. 2, pp. 1023–1086). Elsevier. https://doi.org/10.1016/B978-0-12-824360-2.00027-9

Gasca, J. M. (2015). *Aportaciones al conocimiento sobre los dinosaurios del Barremiense inferior (Cretácico Inferior) de Teruel, España: asociaciones fósiles, sistemática, paleodiversidad y afinidades paleobiogeográficas*. Ph.D. thesis, Universidad of Zaragoza

Góczán, F., & Juhász, M. (1984). Monosulcate pollen grains of angiosperms from Hungarian Albian sediments I. *Acta Botanica Hungarica, 30*, 289–319.

Grimm, E. C. (1992). *Tilia, version 2*. Illinois State Museum, Research and Collection Center, Springfield, USA.

Grimm, E. C. (2004). *TGView, version 2.0.2*. Illinois State Museum, Research and Collection Center, Springfield, USA.

Heimhofer, U., & Hochuli, P. A. (2010). Early Cretaceous angiosperm pollen from a low-latitude succession (Araripe Basin, NE Brazil). *Review of Palaeobotany and Palynology, 161*, 105–126. https://doi.org/10.1016/j.revpalbo.2010.03.010

Heimhofer, U., Hochuli, P. A., Burla, S., Dinis, J. M. L., & Weissert, H. (2005). Timing of Early Cretaceous angiosperm diversification and possible links to major paleoenvironmental change. *Geology, 33*(2), 141–144. https://doi.org/10.1130/G21053.1

Heimhofer, U., Hochuli, P. A., Burla, S., & Weissert, H. (2007). New records of Early Cretaceous angiosperm pollen from Portuguese coastal deposits: Implications for the timing of the early angiosperm radiation. *Review of Palaeobotany and Palynology, 144*, 39–76. https://doi.org/10.1016/j.revpalbo.2005.09.006

Herngreen, G. F. W., Kedves, M., Rovnina, L. V., & Smirnova, S. B. (1996). Chapter 29 C. Cretaceous palynofloral provinces: a review. In J. Jansonius, & D. C. McGregor (Eds.), *Palynology: Principles and Applications* (Vol. 3, pp. 1157–1188). American Association of Stratigraphic Palynologists Foundation, Salt Lake City, USA.

Hochuli, P. A., Heimhofer, U., & Weissert, H. (2006). Timing of early angiosperm radiation: Recalibrating the classical succession. *Journal of the Geological Society, London, 163*, 587–594. https://doi.org/10.1144/0016-764905-135

Hotton, C. L., & Baghai-Riding, N. L. (2010). Palynological evidence for conifer dominance within a heterogeneous landscape in the Late Jurassic Morrison Formation, U.S.A. In C. T. Gee (Ed.), *Plants in Mesozoic time: Morphological innovations, phylogeny, ecosystems* (pp. 295–328). Indiana University Press.

Hughes, N. F., & McDougall, A. B. (1990). Barremian—Aptian angiospermid pollen records from southern England. *Review of Palaeobotany and Palynology, 65*, 145–151. https://doi.org/10.1016/0034-6667(90)90065-Q

Ibáñez, A., Soria, A. R., & Liesa, C. L. (2015). Sedimentology and sedimentary evolution of the Artoles Fm in Miravete de la Sierra (Teruel, Iberian Chain). *Geogaceta, 58*, 11–14.

Ibrahim, M. I. A. (2002). New angiosperm pollen from the upper Barremian—Aptian of the Western Desert. *Egyptian Palynology, 26*, 107–133. https://doi.org/10.1080/01916122.2002.9989569

Illueca, N., Liesa, C. L., & Soria, A. R. (2023). Ciclicidad climática en sedimentos lacustres de la Formación El Castellar (Cretácico inferior, Cordillera Ibérica). *Geogaceta, 74*, 3–6.

Illueca, N., Liesa, C. L., & Soria, A. R. (2024). Linking high-frequency lacustrine sequences to orbitally-induced cyclicity (Lower Cretaceous, Iberian Basin). *Geologica Acta, 22*, 1–26. https://doi.org/10.1344/GeologicaActa2024.22.10

Jarzen, D. M., & Nichols, D. J. (1996). Chapter 9. Pollen. In J. Jansonius, & D. C. McGregor (Eds.), *Palynology: principles and applications* (Vol. 1, pp. 261–291). American Association of Stratigraphic Palynologists Foundation, Salt Lake City, USA.

Kvaček, J., Doyle, J. A., Endress, P. K., Daviero-Gomez, V., Gomez, B., & Tekleva, M. (2016). *Pseudoasterophyllites cretaceous* from the Cenomanian (Cretaceous) of the Czech Republic: A possible link between Chloranthaceae and *Ceratophyllum*. *Taxon, 65*(6), 1345–1373. https://doi.org/10.12705/656.8

Kvaček, J., Gomez, B., & Zetter, R. (2012). The early angiosperm *Pseudoasterophyllites cretaceus* from Albian-Cenomanian of the Czech Republic and France revisited. *Acta Palaeontologica Polonica, 57*(2), 437–443. https://doi.org/10.4202/app.2009.0060

Leereveld, H., de Haan, P. J., & Juhász, M. (1989). Stratigraphic evaluation of spore/pollen assemblages from the Lower Cretaceous of the Alpine-Mediterranean Realm. *Laboratory of Palaeobotany and Palynology Contributions series*, *89*/07, 1–253, 251–298.

Liesa, C., Soria, A. R., & Meléndez, A. (2000). Lacustrine evolution in a basin controlled by extensional faults: the Galve subbasin, Teruel, Spain. In E. H. Gierlowski-Kordesch & K. R. Kelts (Eds.), *Lake Basins through Space and Time*. American Association of Petroleum Geologists, Studies in Geology, *46*, 295–302.

Liesa, C. L., Casas, A. M., Soria, A. R., Simón, J. L., & Meléndez, A. (2004). Estructura extensional cretácica e inversión terciaria en la región Aliaga-Montalbán. In F. Colombo, C. L. Liesa, G. Meléndez, A. Pocoví, C. Sancho, & A. R. Soria (Eds.), *Itinerarios Geológicos por Aragón*. Geo-Guías, *1*, 151–180.

Liesa, C. L., Soria, A. R., Casas, A., Aurell, M., Meléndez, N., Bádenas, B., Fregenal-Martínez, M., Navarrete, R., Peropadre, C.,

& Rodríguez-López, J. P. (2019). The South-Iberian, Central Iberian and Maestrazgo Basins. In J. T. Oliveira, & C. Quesada (Eds.), *The Geology of Iberia: A geodynamic Approach. Volume 3: the Alpine Cycle* (pp. 214–228). Springer.

Liesa, C. L., Casas, A. M., & Simón, J. L. (2018). La tectónica de inversión en una región intraplaca: la Cordillera Ibérica. *Revista de la Sociedad Geológica de España, 31*, 23–50.

Liesa, C. L., Casas-Sainz, A. M., Aurell, M., Simón, J. L., & Soria, A. R. (2023). Salt tectonics *vs* inversion tectonics: The anticlines of the western Maestrazgo revisited (eastern Iberian Chain, Spain). *Basin Research, 35*(1), 295–335. https://doi.org/10.1111/bre.12713

Liesa, C. L., Soria, A. R., Meléndez, N., & Meléndez, A. (2006). Extensional fault control on the sedimentation patterns in a continental rift basin: El Castellar Formation, Galve sub-basin, Spain. *Journal of the Geological Society of London, 163*, 487–498. https://doi.org/10.1144/0016-764904-169

Lopes, F. D. S. (2018). *Calibration of the West African palynological zonation at the Barremian–Aptian boundary with isochronous marine sequences from the Maestrat Basin (Province of Teruel, Spain)*. M.Sc. thesis, University of Perugia.

Martín-Chivelet, J., Berástegui, X., Rosales, I., Vera, J. A., Vilas, L., Caus, E., Gräfe, K.-U., Segura, M., Puig, C., Mas, R., Robles, S., Floquet, M., Quesada, S., Ruiz-Ortiz, P. A., Fregenal-Martínez, M. A., Salas, R., García, A., Martín-Algarra, A., Arias, C., & Ortega, F. (2002). Cretaceous. In W. Gibbons & T. Moreno (Eds.), *The Geology of Spain* (pp. 255–292). The Geological Society of London.

Martín-Closas, C. (1989). *Els carófits del Cretaci Inferior de les conques perifèriques del Bloc de l'Ebre*. Ph.D. thesis, Universitat de Barcelona.

Médus, J. (1970). A palynological method for stratigraphical correlations. A study of the Barremian, Aptian and Albian Complex of North-Eastern Spain and of Roussillon in France. *Grana, 10*, 149–158.

Meléndez, N., Liesa, C. L., Soria, A. R., & Meléndez, A. (2009). Lacustrine system evolution during early rifting: El Castellar Formation (Galve sub-basin, Central Iberian Chain). *Sedimentary Geology, 222*, 64–77. https://doi.org/10.1016/j.sedgeo.2009.05.019

Mendes, M. M., Barrón, E., Dinis, P., Rey, J., & Batten, D. J. (2018). A new palynoflora from upper Barremian–lower Aptian rocks at Casal do Borracho, Torres Vedras, western Portugal, and its palaeoecological significance. *Cretaceous Research, 90*, 363–374. https://doi.org/10.1016/j.cretres.2018.06.012

Mendes, M., Descamps, G. S., Fernandes, P., Lopes, G., Jorge, R. C. G. S., & Pereira, Z. (2023). The upper Hauterivian—Barremian (Lower Cretaceous) Arrifes section (Algarve Basin, Southern Portugal): A palynostratigraphic and palaeoenvironmental approach. *Cretaceous Research, 144*, Article 105433. https://doi.org/10.1016/j.cretres.2022.105433

Mohr, B. A. R. (1987). Mikrofloren aus vertebraten-führenden unterkreide-schichten bei Galve und Uña (Ostspanien). *Berliner Geowissenschalfliche Abhandlungen A, 86*, 69–85.

Mohr, B. A. R. (1989). New palynological information on the age and environment of Late Jurassic and Early Cretaceous vertebrate localities of the Iberian Peninsula (eastern Spain and Portugal). *Berliner Geowissenschalfliche Abhandlungen A, 106*, 291–301.

Najarro, M., Rosales, I., Moreno-Bedmar, J. A., de Gea, G. A., Barrón, E., Company, M., & Delanoy, G. (2011). High-resolution chemo- and biostratigraphic records of the Early Aptian oceanic anoxic event in Cantabria (N Spain): Palaeoceanographic and palaeoclimatic implications. *Palaeogeography, Palaeoclimatology, Palaeoecology, 299*, 137–158. https://doi.org/10.1016/j.palaeo.2010.10.042

Navarrete, R. (2015). *Controles alocíclicos de la sedimentación Barremiense (Formación Camarillas) en el margen occidental de la Cuenca del Maestrazgo*. Ph.D. thesis, Universidad de Zaragoza.

Navarrete, R., Liesa, C. L., Castanera, D., Soria, A. R., Rodríguez-López, J. P., & Canudo, J. I. (2014). A thick Tethyan multi-bed tsunami deposit preserving a dinosaur megatracksite within a coastal lagoon (Barremian, eastern Spain). *Sedimentary Geology, 313*, 105–127. https://doi.org/10.1016/j.sedgeo.2014.09.007

Navarrete, R., Liesa, C. L., Soria, A. R., & Rodríguez-López, J. P. (2013a). Actividad de fallas durante el depósito de la Formación Camarillas (Barremiense) en la subcuenca de Galve (E de España). *Geogaceta, 53*, 61–64.

Navarrete, R., Rodríguez-López, J. P., Liesa, C. L., Soria, C. L., & Veloso, F. M. L. (2013b). Changing physiography of rift basins as a control on the evolution of mixed siliciclastic–carbonate back-barrier systems (Barremian Iberian Basin, Spain). *Sedimentary Geology, 289*, 40–61. https://doi.org/10.1016/j.sedgeo.2013.02.003

Pais, J., & Reyre, Y. (1980–1981). Problèmes posés par la population sporo-pollinique d'un niveau à plantes de la série de Buarcos (Portugal). *Boletim da Sociedade Geológica de Portugal*, *22*, 35–40.

Pérez-Loinaze, V. S., Vera, E. I., Moyano-Paz, D., Coronel, M. D., Manabe, M., Tsuihiji, T., & Novas, F. E. (2023). Maastrichtian palynological assemblages from the Chorrillo Formation, Patagonia, Argentina. *Review of Palaeobotany and Palynology, 314*, Article 104893. https://doi.org/10.1016/j.revpalbo.2023.104893

Peropadre, C. (2012). *El Aptiense del margen occidental de la cuenca del Maestrazgo: controles tectónico, eustático y climático en la sedimentación*. Ph.D. thesis, Universidad Complutense de Madrid.

Peropadre, C., Meléndez, N., & Liesa, C. L. (2007). Heterogeneous subsidence and paleogeographic elements in an extensional setting revealed through the correlation of a storm deposit unit (Aptian, E Spain). *Journal of Iberian Geology, 33*, 79–91.

Peropadre, C., Meléndez, N., & Liesa, C. L. (2008). Variaciones del nivel mar registradas como valles incisos en la Formación Villarroya de los Pinares en la subcuenca de Galve (Teruel, Cordillera Ibérica). *Geo-Temas, 10*, 167–170.

Peropadre, C., Meléndez, N., & Liesa, C. L. (2013). High-frequency, moderate to high-amplitude sea-level oscillations during the late early Aptian: Insights into the mid-Aptian event (Galve Subbasin, Spain). *Sedimentary Geology, 294*, 233–250. https://doi.org/10.1016/j.sedgeo.2013.05.019

Peyrot, D., Playford, G., Mantle, D. J., Backhouse, J., Milne, L. A., Carpenter, R. J., Foster, C., Mory, A. J., McLoughlin, S., Vitacca, J., Scibiorski, J., Mack, C. L., & Bevan, J. (2019). The greening of Western Australian landscapes: The Phanerozoic plant record. *Journal of the Royal Society of Western Australia, 102*, 52–82.

Peyrot, D., Rodríguez-López, J. P., Lassaletta, L., Meléndez, N., & Barrón, E. (2007). Contributions to the palaeoenvironmental knowledge of the Escucha Formation in the Lower Cretaceous Oliete Sub-basin, Teruel, Spain. *Comptes Rendus Palevol, 6*, 469–481. https://doi.org/10.1016/j.crpv.2007.09.014

Pillon, Y. (2012). Time and tempo of diversification in the flora of New Caledonia. *Botanical Journal of the Linnean Society, 170*, 288–298. https://doi.org/10.1111/j.1095-8339.2012.01274.x

Pons, D., Masure, E., Canudo, J. I., Sánchez-Pellicer, R., & Díez, J. B. (2013). Datation palynologiques des formations Camarillas et Artoles dans le Synclinal de Galve, Province de Teruel, Espagne. In B. Cascales-Miñana, U. Villanueva-Amadoz & J. B. Díez (Eds.), *Proceedings of the II Agora Paleobotanica Meeting 9–13/7/2013, Ariño (Teruel). A Congress in the Countryside* (pp. 38–39). Zaragoza.

Regali, M. S. P. (1989). *Tucanopollis*, um gênero novo das angiospermas primitivas. *Boletim de Geociências de Petrobrás, 3*, 395–402.

Regali, M. S. P., Uesugui, N., & Santos, A. S. (1974). Palinologia dos sedimentos meso-cenozóicos do Brazil. *Boletim Tecnico Da Petrobrás, 17*, 117–191.

Riveline, J., Berger, J. P., Feist, M., Martín-Closas, C., Schudack, M., & Soulié-Märsche, I. (1996). European Mesozoic—Cenozoic charophyte biozonation. *Bulletin de la Société Géologique de France, 167*(3), 453–468.

Rodríguez-Barreiro, I., Santos, A. A., Villanueva-Amadoz, U., Gasulla, J. M., Escaso, F., Ortega, F., Gee, C. T., & Díez, J. B. (2024). Palynological reconstruction of the habitat and diet of *Iguanodon bernissartensis* in the Lower Cretaceous Morella Formation, NE Iberian Peninsula. *Cretaceous Research, 156*, Article 105804. https://doi.org/10.1016/j.cretres.2023.105804

Rodríguez López, J. P. (2008). *Sedimentología y evolución del sistema desértico arenoso (erg) desarrollado en el margen occidental del Tethys durante el Cretácico Medio, Cordillera Ibérica. Provincias de Teruel y Zaragoza*. Ph.D. thesis, Universidad Complutense de Madrid.

Rodríguez-López, J. P., Meléndez, M. N., Soria, A. R., & de Boer, P. L. (2009). Reinterpretación estratigráfica y sedimentológica de las formaciones Escucha y Utrillas de la Cordillera Ibérica. *Revista de la Sociedad Geológica de España, 22*(3–4), 163–219.

Ruiz-Omeñaca, J. I., Canudo, J. I., Aurell, M., Badenas, B., Cuenca-Bescós, G., & Ipas, J. (2004). Estado de las investigaciones sobre los vertebrados del Jurásico Superior y el Cretácico Inferior de Galve (Teruel). *Estudios Geológicos, 60*, 179–202. https://doi.org/10.3989/egeol.04603-694

Salas, R. (1987). *El Malm y el Cretaci Inferior entre el Massis de Garraf y la Serra d´Espadà*. Ph.D. thesis. Universitat de Barcelona.

Salas, R., Guimerà, J., Más, R., Martín-Closas, C., Meléndez, A., & Alonso, A. (2001). Evolution of the Mesozoic Central Iberian Rift System and its Cenozoic inversion (Iberian Chain). In P. A. Ziegler, W. Cavazza, A. F. H. Robertson, & S. Crasquin-Soleau (Eds.), *Peri-Tethys Memoir 6: PeriTethyan Rift/Wrench Basins and Passive Margins*. Mémoires du Muséum National d'Histoire Naturelle, Paris, *186*, 145–185.

Salas, R., & Casas, A. (1993). Mesozoic extensional tectonics, stratigraphy and crustal evolution during the Alpine cycle of the eastern Iberian basin. *Tectonophysics, 228*, 33–55. https://doi.org/10.1016/0040-1951(93)90213-4

Salas, R., Martín-Closas, C., Querol, X., Guimerà, J., & Roca, E. (1995). El Cretácico inferior del Nordeste de Iberia. In R. Salas & C. Martín-Closas (Eds.), *Evolución tectosedimentaria de las cuencas del Maestrazgo y Aliaga-Penyagolosa durante el Cretácico Inferior* (pp. 13–94). Universitat de Barcelona.

Schudack, U., & Schudack, M. (2009). Ostracod biostratigraphy in the Lower Cretaceous of the Iberian Chain (eastern Spain). *Journal of Iberian Geology, 35*, 141–168.

Simón, J. L., & Liesa, C. L. (2011). Incremental slip history of a thrust: diverse transport directions and internal holding of the Utrillas thrust sheet (NE Iberian Chain, Spain). In J. Poblet, J., & R. J. Lisle (Eds.), *Kinematic evolution and structural styles of fold-and-thrust belts*. The Geological Society of London, Special Publication, *349*, 77–97. https://doi.org/10.1144/SP349.5

Solé de Porta, N., & Salas, R. (1994). Conjuntos microflorísticos del Cretácico Inferior de la Cuenca del Maestrazgo. Cordillera Ibérica Oriental (NE de España). *Cuadernos de Geología Ibérica, 18*, 355–368.

Soria, A. R. (1997). *La sedimentación en las cuencas marginales del surco ibérico durante el Cretácico Inferior y su control estructural*. Ph.D. thesis, Universidad de Zaragoza.

Soria, A. R., Meléndez, M. N., Meléndez, A., Liesa, C. L., Aurell, M., & Goméz-Fernández, J. C. (2000). The Early Cretaceous of the Iberian Basin (Northeastern Spain). In E. H. Gierlowski-Kordesch, & K. R. Kelts (eds.), *Lake Basins through Space and Time*. American Association of Petroleum Geologists, Studies in Geology, *46*, 285–294.

Soria, A. R., Liesa, C. L., Meléndez, A., & Meléndez, M. N. (2001). Sedimentación sintectónica de la Fm. El Castellar (Cretácico Inferior) en la Subcuenca de Galve (Cuenca Ibérica). *Geo-Temas, 3*, 257–260.

Soria, A. R., Liesa, C. L., Navarrete, R., & Rodríguez-López, J. P. (2023). Sedimentology and stratigraphic architecture of Barremian synrift barrier island-estuarine depositional systems from blended field- and drone-derived data. *Sedimentology, 70*(6), 1812–1855. https://doi.org/10.1111/sed.13097

Sousa, V. A., & Hattemer, H. H. (2003). Pollen dispersal and gene flow by pollen in *Araucaria angustifolia*. *Australian Journal of Botany, 51*, 309–317. https://doi.org/10.1071/BT02037

Taugourdeau-Lantz, J. (1988). Stratigraphic implications of Early Cretaceous spores and pollen grains at holes 638B, 638C, and 641C, Leg 103, off the Iberian Margin, eastern North Atlantic. *Proceedings of the Ocean Drilling Program, Scientific Results, 103*, 419–428. https://doi.org/10.2973/odp.proc.sr.103.151.1988

Tosolini, A., McLoughlin, S., Wagstaff, B., Cantrill, D., & Gallagher, S. (2015). Cheirolepidiacean foliage and pollen from Cretaceous high-latitudes of southeastern Australia. *Gondwana Research, 27*, 960–977. https://doi.org/10.1016/j.gr.2013.11.008

Traverse, A. (2007). *Paleopalynology* (2nd ed.). Springer.

Trincão, P. R. (1990). *Esporos e granos de polen do Cretácico Inferior (Berriasiano-Aptiano) de Portugal: Paleontología e Biostratigrafia*. Ph.D. thesis, Universidade Nova de Lisboa.

Villanueva-Amadoz, U., Santisteban, C., & Santos-Cubedo, A. (2014). Age determination of the Arcillas de Morella Formation (Maestrazgo Basin, Spain). *Historical Biology: An International Journal of Paleobiology, 27*(3–4), 430–441. https://doi.org/10.1080/08912963.2013.874422

Villanueva-Amadoz, U., Sender, L. M., Royo-Torres, R., Verdú, F. J., Pons, D., Alcalá, L., & Díez, J. B. (2015). Palaeobotanical remains associated with dinosaur fossils from the Camarillas Formation (Barremian) of Galve (Teruel, Spain). *Historical Biology: An International Journal of Paleobiology, 27*(3–4), 374–388. https://doi.org/10.1080/08912963.2014.9313857

Wagstaff, B. E., Gallagher, S. J., & Lanigan, K. P. (2006). Late Cretaceous palynological correlation and environmental analyses of fluvial reservoir facies of the Tuna Field, Gippsland Basin, Southeast Australia. *Review of Palaeobotany and Palynology, 138*, 165–186. https://doi.org/10.1016/j.revpalbo.2005.11.002

Watson, J. (1988). The Cheirolepidiaceae. In C. B. Beck (Ed.), *Origin and evolution of gymnosperms* (pp. 382–447). Columbia University Press.